1968

Application of invariant imbedding to radiation transport theory

John Lou Ridihalgh
Iowa State University

APPLICATION OF INVARIANT IMBEDDING TO RADIATION TRANSPORT THEORY

by

John Lou Ridihalgh

A Dissertation Submitted to the
Graduate Faculty in Partial Fulfillment of
The Requirements for the Degree of
DOCTOR OF PHILOSOPHY

Major Subject: Nuclear Engineering

Approved:

Signature was redacted for privacy.

In Charge of Major Work

Signature was redacted for privacy.

Head of Major Department

Signature was redacted for privacy.

Dean of Graduate College

Iowa State University
Ames, Iowa

1968

TABLE OF CONTENTS

	Page
CHAPTER ONE. INTRODUCTION	1
CHAPTER TWO. REVIEW OF THE LITERATURE	4
CHAPTER THREE. THEORY	6
Introduction	6
Invariant Imbedding Equations	7
Gamma Transport	18
Equations for Monoenergetic Radiation Transport	20
CHAPTER FOUR. NUMERICAL SOLUTION OF EQUATIONS	24
Equations for Monoenergetic Radiation Transport	24
Gamma Transport Equations	26
Differential Scattering Cross Section	30
Calculation of Transmitted Flux	32
Energy Buildup Factor	34
Numerical Integration Method	35
Computer Code	39
CHAPTER FIVE. APPLICATIONS	43
Introduction	43
Radiative Transport Stellar Atmospheres	44
Typical reflection functions	45
Comparison with Ambarzumian's results	45
Comparison with Bellman's results	50
Comparison with Chandrasekhar's results	51
Numerical stability of predictor-corrector method	55
Critical Size Problem	56

Page

Gamma Transport Problem 57

Differential energy spectrums 63
Energy buildup factors 71
Evaluation of the numerical method 79

CHAPTER SIX. SUMMARY 80

BIBLIOGRAPHY 82

ACKNOWLEDGEMENT 85

CHAPTER ONE. INTRODUCTION

The classical approach to the particle transport problem has been to examine the behavior of the particles densities within the medium. This approach leads to the Boltzman transport equation. Difficulty is encountered in dealing with this two-point boundary value problem, both in establishing existance and uniqueness of solutions and in obtaining computational solutions. Due to the importance of the transport problem, a great deal of work has been done to find practical numerical procedures for solving the Boltzman equation. The most successful of these have been various forms of direct numerical integration such as the P_N and S_N methods. The Monte Carlo method has also been used to solve difficult transport problems, but this method requires a long computation time to obtain satisfactory results. The methods used to integrate the Boltzman equation directly run into computational difficulties because solving this two point boundary value problem requires iterative procedures.

In a paper (1) published in 1943, the astrophysicist Ambarzumian presented a new approach to the mathematical formulation of transport problems. This approach, based on the use of fundamental equations and the physically intuitive principles of invariance, exploited the multi-stage aspect of the physical processes involved. The reflection and transmission of particles from the medium

is studied rather than studying the particles within the medium. Using this method leads to an initial value problem involving a nonlinear integrodifferential equation. This systematic use of invariance concepts and functional equations is called invariant imbedding. Bellman has made a formal definition of this principle of invariant imbedding (5).

> "PRINCIPLE OF INVARIANT IMBEDDING. Given a physical system, S, whose state at any time t is specified by a state vector, x, we consider a process which consists of a family of transformations applied to this vector.
>
> Suitably enlarging the dimension of the original vector by means of additional components, the state vectors are made elements of a space which is mapped into itself by the family of transformations. In this way we obtain an invariant process, by imbedding the original process within a family of processes.
>
> The functional equations governing the new process are the analytic expression of this invariance."

Even though the invariant imbedding approach leads to a relatively complex integrodifferential equation, the initial value problem is much more easily handled on a digital computer than the two-point boundary value problem. Thus this approach leads to an attractive computational technique for nuclear engineering problems where only the conditions at the boundary are required. The application of this technique has been slow. This is due in part to the emphasis in solving transport problems by the other standard techniques.

The objective of this thesis is to develop numerical and computational techniques for solving radiation transport

problems using the invariant imbedding method, and to apply these techniques to calculate energy buildup factors for gamma transport in finite media.

CHAPTER TWO. REVIEW OF THE LITERATURE

The astrophysicist Ambarzumian (1) first systematically used the principles of invariance and functional equations to solve the problem of radiative transport in stellar atmospheres. The ideas of Ambarzumian were further developed and generalized by Chandrasekhar (16) for the problem of radiative transport. These "principles of invariance" of Ambarzumian-Chandrasekhar were extended and generalized by Bellman and Kalaba (5) in 1956 and applied to the study of inhomogeneous regions of plane, cylindrical and spherical type and to stratified regions in general. This general mathematical technique of invariant imbedding became a very popular mathematical subject and a great number of papers appeared in the late 1950's and early 1960's.

The results of invariant imbedding are extensively discussed in an abstract setting by Preisendorfer (21, 22, 23) and many detailed results are given by Ueno (29, 30, 31, 32). Redheffer (27, 28) applied invariant imbedding techniques to scattering problems, electromechanical problems and to transmission line theory. Ramakrishnan (24, 25, 26) applied these techniques to scattering and diffusion theory problems.

The first applications of invariant imbedding to nuclear engineering problems appears in a joint paper by Bellman, Kalaba and Wing (14). In a series of articles Bellman,

Kalaba, and Wing (4, 6, 7, 8, 9, 10, 11, 12, 13) further developed the neutron diffusion and transport theory and gave existence and uniqueness theorems based on simple physical conversion principles. Wing (33) has written an excellent book which compares classical transport theory to invariant imbedding. This book also contains an excellent bibliography.

Although invariant imbedding as a mathematical technique has been extensively explored, little computational work has been done. Ambarzumian and Chandrasekhar report some computational data; however, the use of modern digital computers to solve invariant imbedding equations is reported by Bellman and Kalaba (3). Beisner (2) reports computational results for energy dependent neutron transport problems. Mathews and Hanson (19) have developed a computational scheme for deep penetration of neutrons and Mingle (20) has done computational work for monoenergetic neutron problems.

CHAPTER THREE. THEORY

Introduction

In this chapter a detailed derivation of the invariant imbedding equations in slab geometry is given. These equations were first introduced in the form presented here by Bellman and his co-workers.

Unlike the Boltzman approach to transport theory which is based on the particle or photon flux in the medium, the basic equations of the invariant imbedding approach concern the reflection and transmission functions of the particles or photons. No attempt is made to describe the flux within the medium. Only the particles or photons transmitted through or reflected from boundaries are of interest. In this respect the invariant imbedding method is not applicable to many nuclear engineering problems, however, this method applies well to shielding problems. The gamma shielding problem is treated in detail in this thesis. The general methods used for the gamma problem also apply to neutron transport problems. The problems of radiation transport in stellar atmospheres and monoenergetic neutron criticality are also treated.

The general energy dependent invariant imbedding equations for inhomogeneous media in slab geometry are derived in detail. The form of the equations needed for the

applications reported in this thesis are then deduced from the general equations.

Invariant Imbedding Equations

The general equations are derived for energy dependent photon or particle transport in an inhomogeneous media. These equations are derived directly from physical processes by the so called particle counting method. It is convenient to start with several definitions. A geometrical representation of the reflection function, $R(x;\bar{\Omega},E;\bar{\Omega}_o,E_o)$, and the transmission function $T(x;\bar{\Omega},E;\bar{\Omega}_o,E_o)$ is shown in Figure 1.

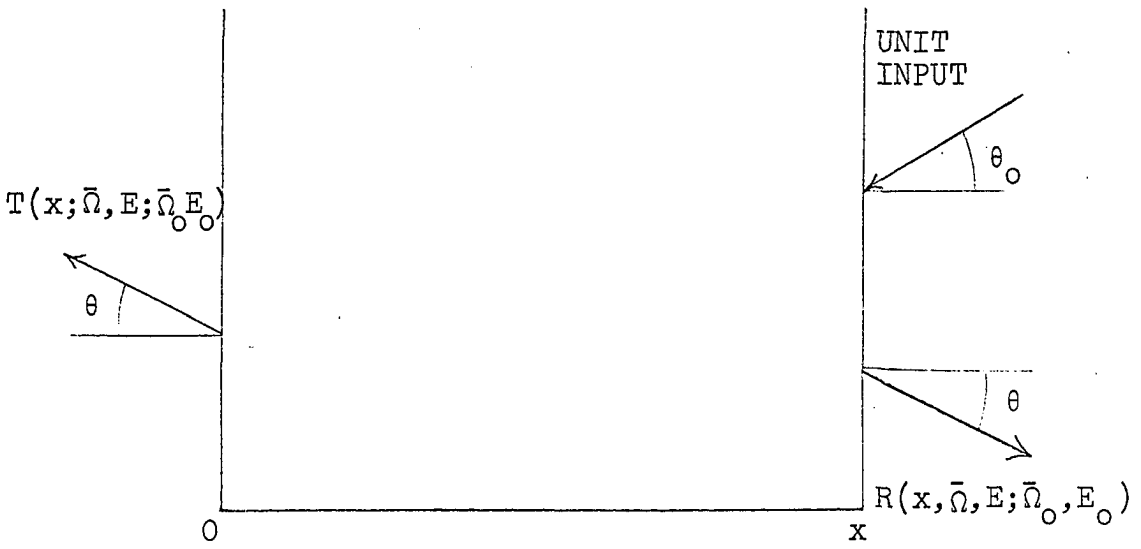

Figure 1. Reflection and transmission functions

$R(x;\bar{\Omega},E;\bar{\Omega}_o,E_o)d\bar{\Omega}dE$ is defined as the number of photons (particles) reflected through a unit area in the exit surface

from a slab of thickness x with energy dE about E and direction $d\bar{\Omega}$ about $\bar{\Omega}$ due to an input of one photon (particle) per second per unit area in the direction $\bar{\Omega}_o$ with energy E_o.

$T(x;\bar{\Omega},E;\bar{\Omega}_o,E_o)d\bar{\Omega}dE$ is defined as the number of photons (particles) transmitted through a unit area of a slab of thickness x with energy dE about E and direction $d\bar{\Omega}$ about $\bar{\Omega}$ due to an input of one photon (particle) per second per unit area in the direction $\bar{\Omega}_o$ with energy E_o.

$K(x;\bar{\Omega},E;\bar{\Omega}_o,E_o)\ d\bar{\Omega}dE$ is defined as the number of photons (particles) transferred into dE about E and $d\bar{\Omega}$ about $\bar{\Omega}$ from energy E_o and direction $\bar{\Omega}_o$ due to an interaction at x.

$\Sigma(x,E)$ is defined as the total macroscopic cross section for interaction with the medium of photons (particles) with energy E.

If a thickness dx is added to the source side of a slab of thickness x having reflection and transmission functions defined as above, the contributions of order dx to the reflection and transmission functions at x+dx are shown in Figures 2 and 3.

The collision probability in dx of a particle entering at x+dx with angle θ_o to the normal is represented as $\Sigma(x,E_o)dx/|\cos\ \theta_o|$, and the mathematical representation of the contributing effects to the reflection function at x+dx can be represented by

$$R(x+dx;\ \bar{\Omega},E;\ \bar{\Omega}_o,E_o)d\bar{\Omega}dE = \sum_{i=1}^{N} R_i \qquad (3.1)$$

where the terms R_i are defined as follows:

$$R_1 = [1 - \Sigma(x,E_o)dx/|\cos\ \theta_o|]R(x;\bar{\Omega},E;\bar{\Omega}_o,E_o)d\bar{\Omega}dE$$

$$x = [1 - \Sigma(x,E)dx/\cos\ \theta] \qquad (3.2)$$

R_1 represents the probability of no interaction in dx followed by reflection in the slab from energy E_o and direction $\bar{\Omega}_o$ into dE about E and $d\bar{\Omega}$ about $\bar{\Omega}$ with no subsequent interaction upon passing through dx.

$$R_2 = [\Sigma(x,E_o)dx/|\cos\ \theta_o|]k(x;\bar{\Omega},E;\bar{\Omega}_o,E_o)d\bar{\Omega}dE \qquad (3.3)$$

R_2 represents the probability of interaction in dx with scattering from energy E_o and direction $\bar{\Omega}_o$ into dE about E and $d\bar{\Omega}$ about $\bar{\Omega}$.

$$R_3 = \int_o^\infty dE' \int_{\bar{\Omega}'in} d\bar{\Omega}'[\Sigma(x,E_o)dx/|\cos\ \theta_o|K(x;\bar{\Omega}',E';\bar{\Omega}_o,E_o)$$

$$x\ \ R(x;\bar{\Omega},E;\bar{\Omega}',E')d\bar{\Omega}dE[1 - \Sigma(x,E')dx/\cos\ \theta] \qquad (3.4)$$

R_3 represents the probability of interaction in dx with scattering from energy E_o and direction $\bar{\Omega}_o$ into some energy dE' about E' and some solid angle $d\bar{\Omega}'$ about $\bar{\Omega}'$ directed inward followed by reflection in the slab into dE about E and $d\bar{\Omega}$ about $\bar{\Omega}$ with no subsequent interaction upon passing

through dx.

$$R_4 = \int_0^\infty dE'' \int_{\bar{\Omega}''\text{out}} d\bar{\Omega}'' [1 - \Sigma(x,E_o)dx/|\cos\ \theta_o|]R(x;\bar{\Omega}'',E';\bar{\Omega}_o,E_o)$$

$$x\ \ [\Sigma(x,E'')dx/\cos\ \theta'']K(x;\bar{\Omega},E;\bar{\Omega}'',E'')d\bar{\Omega}dE \qquad (3.5)$$

R_4 represents the probability of no interaction in dx followed by reflection in the slab from E_o and $\bar{\Omega}_o$ into some dE' about E' and into some $d\bar{\Omega}'$ about $\bar{\Omega}'$ directed outward with subsequent scattering upon reentering dx into $d\bar{\Omega}$ about $\bar{\Omega}$ with energy dE about E.

$$R_5 = \int_0^\infty dE' \int_{\bar{\Omega}'\text{in}} d\bar{\Omega}' \int_0^\infty dE'' \int_{\bar{\Omega}''\text{out}} d\bar{\Omega}'' [1-\Sigma(x,E_o)dx/|\cos\ \theta_o|]$$

$$x\ \ R(x;\bar{\Omega}'',E'';\bar{\Omega}_o,E_o)[\Sigma(x,E'')dx/\cos\ \theta'']K(x;\bar{\Omega}',E';\bar{\Omega}'',E'')$$

$$x\ \ R(x;\bar{\Omega},E;\bar{\Omega}',E')d\bar{\Omega}dE[1-\Sigma(x,E)dx/\cos\ \theta] \qquad (3.6)$$

R_5 represents the probability of no interaction in dx followed by reflection in the slab from E_o and $\bar{\Omega}_o$ into some dE' about E' and into some $d\bar{\Omega}'$ about $\bar{\Omega}'$ directed outward then scattering while reentering dx into some dE'' about E'' and $d\bar{\Omega}''$ about $\bar{\Omega}''$ directed again inward with subsequent reflection into dE about E and $d\bar{\Omega}$ about $\bar{\Omega}$ with no interaction while again passing through dx. All other interactions will lead to terms of second order in dx or higher.

In order to find the reflection function at x $R(x+dx;\bar{\Omega},E;\bar{\Omega}_o,E_o)$ is expanded in a Taylor's series about x and terms of order dx only are retained. Similarily terms of order dx only on the right side of Equation 3.1 are retained. This produces

$$\frac{d}{dx} R(x;\bar{\Omega},E;\bar{\Omega}_o,E_o) = [\Sigma(x,E_o)/|\cos\theta_o|]K(x;\bar{\Omega},E;\bar{\Omega}_o,E_o)$$

$$- [\Sigma(x,E_o)/|\cos\theta_o| + \Sigma(x,E)/\cos\theta]R(x;\bar{\Omega},E;\bar{\Omega}_o,E_o)$$

$$+ \int_o^\infty dE' \int_{\bar{\Omega}'in} d\bar{\Omega}' [\Sigma(x,E_o)/|\cos\theta_o| K(x;\bar{\Omega}',E';\bar{\Omega}_o,E_o)$$

$$x \quad R(x;\bar{\Omega},E;\bar{\Omega}',E) + \int_o^\infty dE'' \int_{\bar{\Omega}''out} d\bar{\Omega}'' R(x;\bar{\Omega}'',E'';\bar{\Omega}_o,E_o)$$

$$x \quad [\Sigma(x,E'')/\cos\theta'']K(x;\bar{\Omega},E;\bar{\Omega}'',E'')$$

$$+ \int_o^\infty dE' \int_{\bar{\Omega}'in} d\bar{\Omega}' \int_o^\infty dE'' \int_{\bar{\Omega}''out} d\bar{\Omega}'' R(x;\bar{\Omega}'',E'';\bar{\Omega}_o,E_o)$$

$$x \quad [\Sigma(x,E'')/\cos\theta'']K(x;\bar{\Omega}',E';\bar{\Omega}'',E'')R(x;\bar{\Omega},E;\bar{\Omega}',E') \tag{3.7}$$

with initial condition

$$R(0;\bar{\Omega},E;\bar{\Omega}_o,E_o) = 0 \tag{3.8}$$

In slab geometry the φ-dependence of the solid angle can be integrated so that

$$d\bar{\Omega} = 2\pi \sin\theta d\theta = -2\pi d\mu \tag{3.9}$$

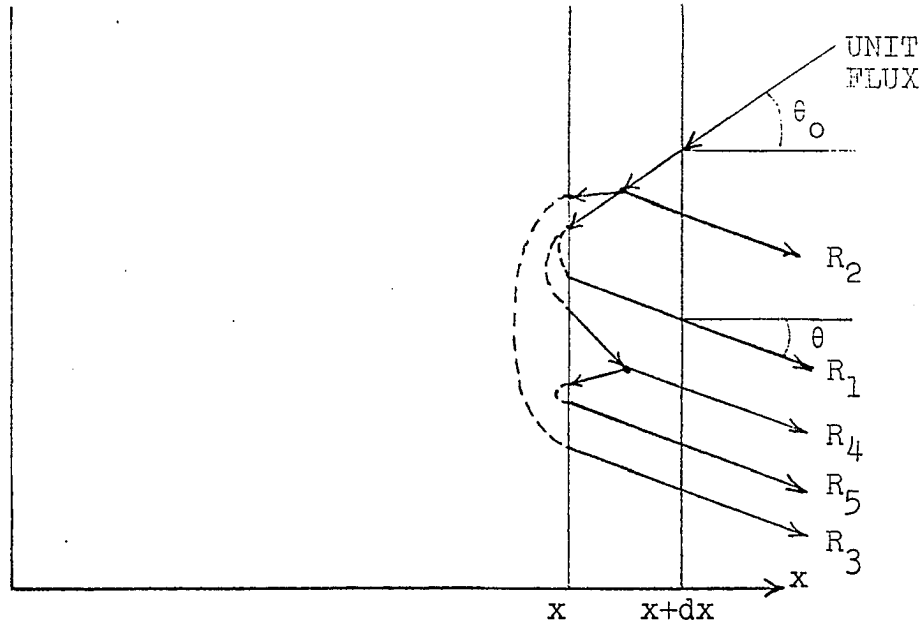

Figure 2. Contributions to reflection function due to a unit flux input at angle θ_o

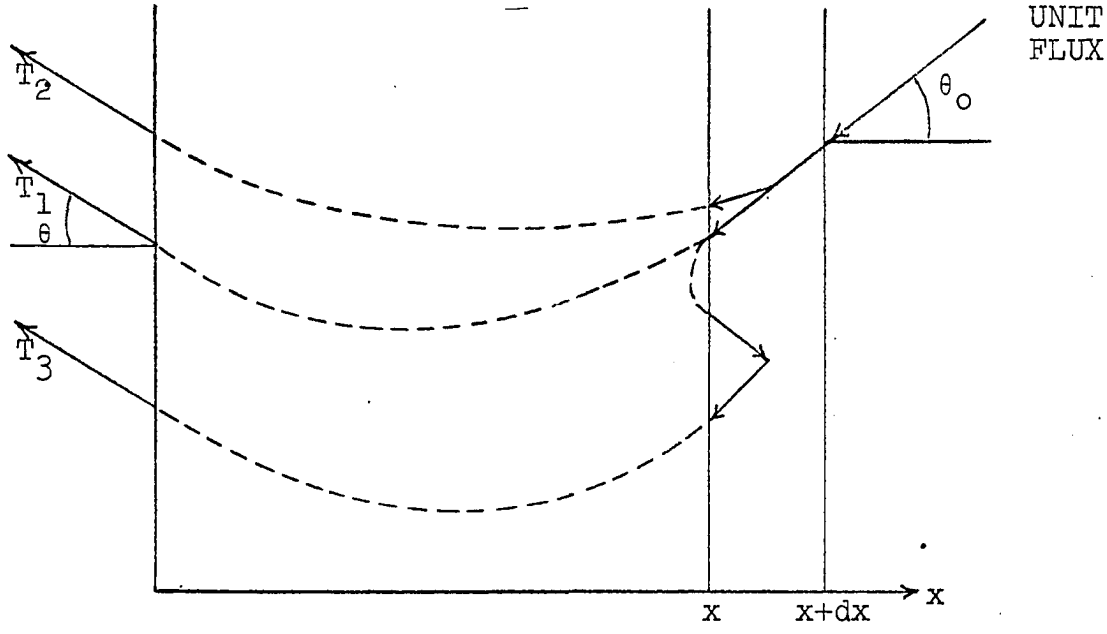

Figure 3. Contributions to transmission function due to a unit flux input at angle θ_o

where $\mu = \cos\theta$. Thus the transformations

$$r(x;\mu,E;\mu_o,E_o) = \frac{\mu_o}{2\pi}\int_o^{2\pi} d\varphi_o \int_o^{2\pi} d\varphi\, R(x;\bar{\Omega},E;\bar{\Omega}_o,E_o) \tag{3.10}$$

$$K(x;\mu,E;\mu_o,E_o) = \int_o^{2\pi} d\varphi_o \int_o^{2\pi} d\varphi\, K(x;\bar{\Omega},E;\bar{\Omega}_o,E_o) \tag{3.11}$$

along with redefining the imput and output θ angles to the slab face in terms of their respective normal conditions give

$$\begin{aligned}
\frac{d}{dx} r(x;\mu,E;\mu_o,E_o) &= \Sigma(x,E_o)K(x;\mu,E;\mu_o,E_o) \\
&- [\Sigma(x,E_o)/\mu_o + \Sigma(x,E)/\mu]r(x;\mu,E;\mu_o,E_o) \\
&+ \int_o^\infty dE' \int_o^1 d\mu'/\mu' \,[\Sigma(x,E_o)]K(x;\mu',E';\mu_o,E_o)R(x;\mu,E;\mu',E') \\
&+ \int_o^\infty dE'' \int_o^1 d\mu''/\mu'' \, r(x;\mu'',E'';\mu_o,E_o)[\Sigma(x,E'')]K(x;\mu,E;\mu'',E'') \\
&+ \int_o^\infty dE' \int_o^1 d\mu'/\mu' \int_o^\infty dE'' \int_o^1 d\mu''/\mu'' \, r(x;\mu'',E'';\mu_o,E_o)\Sigma(x,E'') \\
&\times K(x;\mu',E';\mu'',E'')r(x;\mu,E;\mu',E')
\end{aligned} \tag{3.12}$$

with initial condition

$$r(0;\mu,E;\mu_o,E_o) = 0 \tag{3.13}$$

The transmission function is derived in a similar manner. Figure 2 shows the contributions to the transmission function

at x+dx to order dx. Mathematically the transmission function at x+dx can be represented by

$$T(x+dx;\bar{\Omega},E;\bar{\Omega}_o,E_o)d\bar{\Omega}dE = \sum_{i=1}^{3} T_i \tag{3.14}$$

where the terms T_i represent the following:

$$T_1 = [1-\Sigma(x,E_o)dx/|\cos\ \theta_o|]T(x;\bar{\Omega},E;\bar{\Omega}_o,E_o)d\bar{\Omega}dE \tag{3.15}$$

T_1 represents the probability of no interaction in dx followed by transmission through the slab from energy E_o and direction $\bar{\Omega}_o$ to energy dE about E and into $d\bar{\Omega}$ about $\bar{\Omega}$.

$$T_2 = \int_{\bar{\Omega}'in} d\bar{\Omega}' \int_o^\infty dE' [\Sigma(x,E_o)dx/|\cos\ \theta_o|]K(x;\bar{\Omega}',E';\bar{\Omega}_o,E_o)$$

$$x\ \ T(x;\bar{\Omega},E;\bar{\Omega}_o,E_o)d\bar{\Omega}dE \tag{3.16}$$

T_2 represents the probability of interaction upon entering dx with scattering from energy E_o and direction $\bar{\Omega}_o$ into some energy dE' about E' and some solid angle $d\bar{\Omega}'$ about $\bar{\Omega}'$ into the slab with subsequent transmission through the slab into energy dE about E and $d\bar{\Omega}$ about $\bar{\Omega}$.

$$T_3 = \int_{\bar{\Omega}'in} d\bar{\Omega}' \int_o^\infty dE' \int_{\bar{\Omega}''out} d\bar{\Omega}'' \int_o^\infty dE'' [1-\Sigma(x,E_o)dx/|\cos\ \theta_o|]$$

$$x\ \ R(x;\bar{\Omega}'',E'';\bar{\Omega}_o,E_o)[\Sigma(x,E'')dx/\cos\ \theta'']K(x;\bar{\Omega}',E';\bar{\Omega}'',E'')$$

$$x\ \ T(x;\bar{\Omega},E;\bar{\Omega}',E')d\bar{\Omega}dE \tag{3.17}$$

T_3 represents no interaction upon entering dx followed by reflection back into dx from energy E_o and direction $\bar{\Omega}_o$ to some dE" about E" and into some $d\bar{\Omega}$" about $\bar{\Omega}$" with scattering in dx back into the slab with energy dE' about E' and into $d\bar{\Omega}'$ about $\bar{\Omega}'$; followed by transmission through the slab with energy dE about E and into solid angle $d\bar{\Omega}$ about $\bar{\Omega}$.

By expanding $T(x+dx;\bar{\Omega},E;\bar{\Omega}_o,E_o)$ in a Taylor's series about x and retaining only terms of order dx, Equation 3.14 becomes

$$\frac{d}{dx} T(x;\bar{\Omega},E;\bar{\Omega}_o,E_o) = -[\Sigma(x,E_o)/|\cos\theta_o|]T(x;\bar{\Omega},E;\bar{\Omega}_o,E_o)$$

$$+ \int_o^\infty dE' \int_{\bar{\Omega}'in} d\bar{\Omega}' [\Sigma(x,E_o)/|\cos\theta_o|]K(x;\bar{\Omega}',E';\bar{\Omega}_o,E_o)$$

$$x \quad T(x;\bar{\Omega},E;\bar{\Omega}_o,E_o) + \int_o^\infty dE' \int_{\bar{\Omega}'in} d\bar{\Omega}' \int_{\bar{\Omega}'out} d\bar{\Omega}'' \; R(x;\bar{\Omega}'',E'';\bar{\Omega}_o,E_o)$$

$$x \quad [\Sigma(x,E'')/\cos\theta'']K(x;\bar{\Omega}',E';\bar{\Omega}'',E'')T(x;\bar{\Omega},E;\bar{\Omega}',E') \tag{3.18}$$

with initial condition

$$T(0;\bar{\Omega},E;\bar{\Omega}_o,E_o) = \delta(\bar{\Omega}\cdot\bar{\Omega}_o - 1)\delta(E-E_o) \tag{3.19}$$

The φ-dependence of the solid angle can be integrated so that

$$d\bar{\Omega} = 2\pi \sin\theta d\theta = -2\pi d\mu \tag{3.20}$$

where $\mu = \cos\theta$. When the transformations 3.21, 3.22 and 3.10 are applied to Equation 3.18

$$t(x;\mu,E;\mu_o,E_o) = \frac{\mu_o}{2\pi}\int_o^{2\pi} d\varphi_o \int_o^{2\pi} d\varphi\ T(x;\bar{\Omega},E;\bar{\Omega}_o,E_o) \qquad (3.21)$$

$$k(x;\mu,E;\mu_o,E_o) = \int_o^{2\pi} d\varphi_o \int_o^{2\pi} d\varphi\ K(x;\bar{\Omega},E;\bar{\Omega}_o,E_o) \qquad (3.22)$$

$$r(x;\mu,E;\mu_o,E_o) = \frac{\mu_o}{2\pi}\int_o^{2\pi} d\varphi_o \int_o^{2\pi} d\varphi\ R(x;\bar{\Omega},E;\bar{\Omega}_o,E_o) \qquad (3.10)$$

the transmission function becomes

$$\frac{d}{dx}\, t(x;\mu,E;\mu_o,E_o) = -[\Sigma(x,E_o)/\mu_o]t(x;\mu,E;\mu_o,E_o)$$

$$+ \int_o^{\infty} dE' \int_o^{1} d\mu'/\mu'[\Sigma(x,E_o)]k(x;\mu',E';\mu_o,E_o)t(x;\mu,E;\mu',E')$$

$$+ \int_o^{\infty} dE' \int_o^{1} d\mu'/\mu' \int_o^{\infty} dE'' \int_o^{1} d\mu''/\mu''\ r(x;\mu'',E'';\mu_o,E_o)\Sigma(x,E'')$$

$$x\ \ k(x;\mu',E';\mu'',E'')T(x;\mu,E;\mu',E') \qquad (3.23)$$

with initial condition

$$t(0;\mu,E;\mu_o,E_o) = \delta(\mu-\mu_o)\delta(E-E_o)$$

It is advantageous to eliminate the delta function initial condition. This is done by separating the transmission function into a scattered and unscattered portion by letting

$$t(x;\mu,E;\mu_o,E_o) = t^u(x;\mu,E;\mu_o,E_o)\delta(\mu-\mu_o)\delta(E-E_o)$$

$$+ t^s(x;\mu,E;\mu_o,E_o) \qquad (3.24)$$

Substitution of Equation 3.24 into Equation 3.23 and performing the integrations over the unscattered portions represented by the delta functions produces the equations

$$\frac{d}{dx}\, t^u(x;\mu_o,E_o;\mu_o,E_o) = -t^u(x;\mu_o,E_o;\mu_o,E_o)/\mu_o \tag{3.25}$$

$$\begin{aligned}\frac{d}{dx}\, t^u(x;\mu,E;\mu_o,E_o) &= -[\Sigma(x,E_o)/\mu_o]t^s(x;\mu,E;\mu_o,E_o) \\ &+ \Sigma(x,E_o)k(x;\mu,E;\mu_o,R_o)t^u(x;\mu,E;\mu,E) \\ &+ \int_o^\infty dE' \int_o^1 d\mu'/\mu'\Sigma(x,E_o)k(x;\mu',E';\mu_o,E_o)t^s(x;\mu,E;\mu',E') \\ &+ \int_o^\infty dE' \int_o^1 d\mu'/\mu' \int_o^\infty dE'' \int_o^1 d\mu''/\mu'' \; r(x;\mu'',E'';\mu_o,E_o)\Sigma(x,E') \\ &\times \; k(x;\mu',E';\mu'',E'')t^s(x;\mu,E;\mu',E') \\ &+ \int_o^\infty dE'' \int_o^1 d\mu''/\mu'' \; r(x;\mu'',E'';\mu_o,E_o)\Sigma(x,E'')k(x;\mu,E;\mu'',E'') \\ &\times \; t^u(x;\mu,E;\mu,E)\end{aligned} \tag{3.26}$$

with initial conditions

$$t^u(0;\mu,E;\mu,E) = 1 \tag{3.27}$$

$$t^s(0;\mu,E;\mu_o,E_o) = 0 \tag{3.28}$$

Equation 3.25 can be easily integrated

$$t^u(x;\mu,E;\mu,E) = \exp[-(1/|\mu|)\int_o^x \Sigma(s,E)ds] \tag{3.29}$$

For homogeneous slabs this reduces to

$$t^u(x;\mu,E;\mu,E) = \exp[-\Sigma(E)x/\mu] \tag{3.30}$$

For the case of multilayered slabs with constant cross sections within each layer the unscattered component becomes

$$t^u(x;\mu,E;\mu,E) = \exp[-(1/|\mu|)\sum_{i=1}^{N}\Sigma_i(E)x_i] \tag{3.31}$$

where N is the number of regions and x_i is the thickness of the ith region.

Gamma Transport

In order to evaluate Equations 3.12 and 3.26 for the gamma transport problem it is necessary to have an expression for the scattering probability $k(x;\mu,E;\mu_o,E_o)$. For the gamma ray problem

$$k(x;\mu,E;\mu_o,E_o) = \frac{\sigma(\theta)d\bar{\Omega}}{\Sigma(x,E)} \tag{3.32}$$

where $\sigma(\theta)d\bar{\Omega}$ is the differential scattering cross section. Expressed in Thompson units, this cross section is given by the Klien-Nishina formula.

$$\sigma(\theta)d\bar{\Omega} = \frac{3}{16\pi}\frac{\lambda^2}{\lambda^{12}}\left(\frac{\lambda}{\lambda'} + \frac{\lambda'}{\lambda} - \sin^2\theta\right)d\bar{\Omega} \tag{3.33}$$

$\Sigma(x,E)$ is now defined as the total attenuation coefficient for gamma rays of energy E. Since the terms $\Sigma(x,E)k(x;\mu,E;\mu_o,E_o)$ occur throughout the energy dependent equations, it is

convenient to define

$$G(x;\mu,E;\mu_o,E_o) = \Sigma(x,E)k(x;\mu,E;\mu_o,E_o)$$

where $G(x;\mu,E;\mu_o,E_o)$ is the differential cross section defined by the Klien-Nishina formula. Using this notation the reflection function (3.12) becomes

$$\frac{d}{dx} r(x;\mu,E;\mu_o,E_o) = G(x;\mu,E;\mu_o,E_o) - [\Sigma(x,E_o)/\mu_o + \Sigma(x,E)/\mu]$$

$$x \quad r(x;\mu,E;\mu_o,E_o) + \int_o^\infty dE' \int_o^1 d\mu/\mu' \; G(x;\mu',E';\mu_o,E_o)$$

$$x \quad r(x;\mu,E;\mu',E') + \int_o^\infty dE'' \int_o^1 d\mu''/\mu'' \; r(x;\mu'',E'',\mu_o,E_o)$$

$$x \quad G(x;\mu,E;\mu'',E'') + \int_o^\infty dE' \int_o^1 d\mu'/\mu' \int_o^\infty dE'' \int_o^1 d\mu''/\mu''$$

$$x \quad r(x;\mu'',E'';\mu,E)G(x';\mu',E';\mu'',E'')r(x;\mu,E;\mu',E') \tag{3.34}$$

with initial condition

$$r(0;\mu,E;\mu_o,E_o) = 0 \tag{3.35}$$

Similarly the transmission function becomes

$$\frac{d}{dx} t^s(x;\mu,E;\mu_o,E_o) = -[\Sigma(x,E_o)/\mu_o]t^s(x;\mu,E;\mu_o,E_o)$$

$$+ G(x;\mu,E;\mu_o,E_o)t^u(x,\mu,E;\mu,E)$$

$$+ \int_o^\infty dE' \int_o^1 d\mu'/\mu' \; G(x;\mu',E';\mu_o,E_o)t^s(x;\mu,E;\mu',E')$$

$$+ \int_0^\infty dE' \int_0^1 d\mu'/\mu' \int_0^\infty dE'' \int_0^1 d\mu''/\mu'' \; r(x;\mu'',E'';\mu_o,E_o)$$

$$x \;\; G(x;\mu',E';\mu'',E'')t^s(x;\mu,E;\mu',E')$$

$$+ \int_0^1 d\mu''/\mu'' \int_0^\infty dE' \; r(x;\mu'',E'';\mu_o,E_o)G(x;\mu,E;\mu'',E'')$$

$$x \;\; t^u(x;\mu,E;\mu,E) \tag{3.36}$$

and

$$t^u(x;\mu,E;\mu,E) = \exp[-(1/\mu)\int_0^x \Sigma(s,E)ds] \tag{3.37}$$

with initial conditions

$$t^s(0;\mu,E;\mu_o,E_o) = 0 \tag{3.38}$$

$$t^u(0;\mu,E;\mu,E) = 1 \tag{3.39}$$

This form of the invariant imbedding equations is shown in Chapter Four to be more desirable from the computational standpoint.

Equations for Monoenergetic Radiation Transport

The equations used for the monoenergetic neutron criticality problem and the problem of radiation transport in stellar atmospheres can be deduced from the energy dependent equations. The reflection function, transmission function and scattering probability must first be redefined.

$R(x,\bar{\Omega},\bar{\Omega}_o)d\bar{\Omega}$ is defined as the flux of monoenergetic

particles in the direction $d\bar{\Omega}$ about $\bar{\Omega}$ reflected from a slab of thickness x because of an imput of one particle per second per unit area in the direction $\bar{\Omega}_o$.

$T(x,\bar{\Omega},\bar{\Omega}_o)d\bar{\Omega}$ is defined as the flux of monoenergetic particles in the direction $d\bar{\Omega}$ about $\bar{\Omega}$ transmitted through a slab of thickness x because of an imput of one particle per second per unit area in the direction $\bar{\Omega}_o$.

$K(x,\bar{\Omega},\bar{\Omega}_o)d\bar{\Omega}$ is defined as the probability of scattering into $d\bar{\Omega}$ about $\bar{\Omega}$ from direction $\bar{\Omega}_o$.

In order to take into account the possibility of neutron multiplication another definition is necessary. Let C be defined as the mean number of secondaries per collision. For neutrons

$$C = (\nu\Sigma_f(x) + \Sigma_s(x)/\Sigma(x)$$

where $\Sigma_f(x)$, $\Sigma_s(x)$ and $\Sigma(x)$ are the fission, scattering and total cross sections respectively. The product $C\Sigma(x)$ is the number of particles remaining after a collision in the media. Scattering is assumed to be isotropic. Thus $K(x,\bar{\Omega},\bar{\Omega}_o) = \frac{1}{4\pi}$. Also $\Sigma(x)$ is set equal to unity so that the distance is measured in mean free paths. The reflection then becomes

$$\frac{d}{dx} R(x,\bar{\Omega},\bar{\Omega}_o) = C/4\pi|\cos\ \theta_o| - [1/|\cos\ \theta_o + 1/\cos\ \theta]R(x,\bar{\Omega},\bar{\Omega}_o)$$

$$+ \int_{\bar{\Omega}'\text{in}} d\bar{\Omega}'[C/4\pi|\cos\ \theta_o|]R(x,\bar{\Omega},\bar{\Omega}')$$

$$+ \int_{\bar{\Omega}''\text{out}} d\bar{\Omega}''[C/4\pi \cos\theta'']R(x,\bar{\Omega}'',\bar{\Omega}_o) + \int_{\bar{\Omega}'\text{in}} d\bar{\Omega}' \int_{\bar{\Omega}''\text{out}} d\bar{\Omega}''$$

$$x \; R(x,\bar{\Omega},\bar{\Omega}')[C/4\pi \cos\theta'']R(x,\bar{\Omega}'',\bar{\Omega}_o) \tag{3.40}$$

with initial condition

$$R(0,\bar{\Omega},\bar{\Omega}_o) = 0 \tag{3.41}$$

Similarly the transmission function becomes

$$\frac{d}{dx} T(x,\bar{\Omega},\bar{\Omega}_o) = -[1/|\cos\theta_o|]T(x,\bar{\Omega},\bar{\Omega}_o) + C/4\pi \; |\cos\theta_o|$$

$$x \int_{\bar{\Omega}'\text{in}} d\bar{\Omega}' \; T(x,\bar{\Omega},\bar{\Omega}') + C/4\pi \int_{\bar{\Omega}'\text{in}} d\bar{\Omega}' \int_{\bar{\Omega}''\text{out}} d\bar{\Omega}'' \; T(x,\bar{\Omega},\bar{\Omega}')$$

$$x \; R(x,\bar{\Omega}'',\bar{\Omega}_o)/\cos\theta'' \tag{3.42}$$

with initial condition

$$T(0,\bar{\Omega},\bar{\Omega}_o) = \delta(\bar{\Omega}\cdot\bar{\Omega}_o - 1) \tag{3.43}$$

If the φ-dependence of the solid angle is integrated so that

$$d\bar{\Omega} = 2\pi \sin\theta d\theta = -2\pi d\mu$$

where $\mu = \cos\theta$ and the following transformations are made

$$r(x,\mu,\mu_o) = \frac{\mu_o}{2\pi} \int_o^{2\pi} d\varphi_o \int_o^{2\pi} d\varphi \; R(x,\bar{\Omega},\bar{\Omega}_o) \tag{3.44}$$

$$t(x,\mu,\mu_o) = \frac{\mu_o}{2\pi} \int_o^{2\pi} d\varphi_o \int_o^{2\pi} d\varphi \; T(x,\bar{\Omega},\bar{\Omega}_o) \tag{3.45}$$

$$t(x,\mu,\mu_o) = t^u(x,\mu,\mu_o)\delta(\mu-\mu_o) + t^s(x,\mu,\mu_o) \tag{3.46}$$

the reflection and transmission functions become

$$\frac{d}{dx} r(x,\mu,\mu_o) = -[\frac{1}{\mu} + \frac{1}{\mu_o}]\, r(x,\mu,\mu_o)$$

$$+ \frac{C}{2} [1 + \int_o^1 d\mu'/\mu'\, r(x,\mu,\mu')][1 + \int_o^1 d\mu''/\mu''\, r(x,\mu'',\mu_o)] \tag{3.47}$$

$$r(0,\mu,\mu_o) = 0 \tag{3.48}$$

and

$$\frac{d}{dx} t^s(x,\mu,\mu_o) = -t^s(x,\mu,\mu_o)/\mu_o + C/2[1 + \int_o^1 d\mu''/\mu''\, r(x,\mu'',\mu_o)]$$

$$x\ \ [t^u(x,\mu,\mu)/\mu + \int_o^1 d\mu'/\mu'\, t^s(x,\mu,\mu')] \tag{3.49}$$

$$t^u(x,\mu,\mu) = \exp(-x/\mu_o) \tag{3.50}$$

with initial conditions

$$t^s(0,\mu,\mu_o) = 0 \tag{3.51}$$

$$t^u(0,\mu,\mu_o) = 1 \tag{3.52}$$

Equations 3.47, 3.48 and 3.50 are in the form used for the monoenergetic neutron criticality problem. These equations can also be used for the problem of radiation transport in stellar atmospheres if C is redefined as the fraction of absorbed light which is reradiated. C is then referred to as the single scattering albedo.

CHAPTER FOUR. NUMERICAL SOLUTION OF EQUATIONS

Equations for Monoenergetic Radiation Transport

The equations for the monoenergetic and energy dependent reflection and transmission functions are rigorous but cannot be solved because of the integral terms. The monoenergetic equations are reduced to a form which can be solved by replacing the integrations over the angular variations by a numerical integration formula of the Gauss-Legendre type

$$\int_{-1}^{1} f(x)dx \approx \sum_{k=1}^{N} w_k f(x_k) \tag{4.1}$$

where x_k are the roots of the Nth Legendre polynomial and w_k are the corresponding weights. The angular variations of the reflection and transmission function extend only over the half range so that a transformation produces

$$\int_{o}^{1} f(x)dx \approx \sum_{k=1}^{N} W_k \, f(x'_k) \tag{4.2}$$

where $W_k = w_k/2$ and $x'_k = x_k/2 + \frac{1}{2}$. The final form of the equations is formulated by letting

$$R_{i,j}(x) = r(x,\mu_i,\mu_j) \tag{4.3}$$

$$T^{s}_{i,j}(x) = t^{s}(x,\mu_i,\mu_j) \tag{4.4}$$

$$T^{u}_{i,j}(x) = t^{u}(x,\mu_i,\mu_j) \tag{4.5}$$

The nonlinear integrodifferential equations (3.47, 3.49, 3.50) for monoenergetic reflection and transmission are reduced to a set of ordinary nonlinear differential equations of the form

$$\frac{d}{dx} R_{i,j}(x) = -[\frac{1}{\mu_i} + \frac{1}{\mu_j}] R_{i,j}(x) + (\frac{C}{2})[1+ \sum_{k=1}^{N} W_k R_{i,k}(x)/\mu_k]$$

$$x \quad [1+ \sum_{\ell=1}^{N} W_\ell R_{\ell,j}(x)/\mu_\ell] \tag{4.6}$$

$$R_{i,j}(0) = 0 \tag{4.7}$$

and

$$\frac{d}{dx} T^s_{i,j}(x) = -T^s_{i,j}(x)/\mu_j + (\frac{C}{2})[1+ \sum_{\ell=1}^{N} W_\ell R_{\ell,j}(x)/\mu_\ell]$$

$$x \quad [T^u_{i,i}(x)/\mu_i + \sum_{k=1}^{N} W_k T^s_{i,k}(x)/\mu_k] \tag{4.8}$$

$$T^u_{i,i}(k) = \exp(-x/\mu_i) \tag{4.9}$$

$$T^s_{i,j}(0) = 0 \tag{4.10}$$

$$T^u_{i,i}(0) = 0 \tag{4.11}$$

The order of the set of equations is dependent on the order of approximation of integrations over the angles. The reflection function is symmetric therefore the size of the system of equations is $N(N+1)/2$, where N is the order of the approximation of the integral terms. The transmission function is nonsymmetric and also requires the reflection

function; therefore, the size of the system of equations required is $N^2+N(N+1)/2$. For example, if a quadrature of order seven is used the reflection function requires 28 equations while the transmission function requires 49 + 28 or 77 equations.

In the case of the neutron criticality problem C is the mean number of secondaries per collision, while in the problem of light transport in stellar atmospheres C is the fraction of the absorbed light which is reradiated. Thus Equations 4.6 and 4.8 are in the form used for both mono-energetic problems treated in this thesis.

Gamma Transport Equations

The equations for energy dependent gamma transport require additional approximations over the energy integrals in order to reduce the equations to a form easily solvable by numerical methods. The energy integrals are approximated by dividing the continuous energy spectrum into a number of energy groups. The reflection function from group m to group n is defined by the equation

$$r_{m,n}(x,\mu,\mu_o) = \int_n dE \int_m dE_o \; r(x;\mu,E;\mu_o,E_o) f_m(E_o) \qquad (4.12)$$

where $\int_n dE$ denotes integration over the group n. $f_m(E_o)$ is a suitable weighting function for the group satisfying the condition

$$\int_m f_m(E)dE = 1 \tag{4.13}$$

Similarly, the transmission function from group m to group n is defined by

$$t_{m,n}(x,\mu,\mu_o) = \int_n dE \int_m dE_o t(x;\mu,E;\mu_o,E_o)f_m(E_o) \tag{4.14}$$

When a group approximation to the energy integrals is used an average total cross section for scattering of a group and a group approximation for the differential scattering cross section is required. The average total cross section of the group m is defined by

$$\Sigma_m(x) = \int_m dE\Sigma(x,E)f_m(E) \tag{4.15}$$

The differential scattering cross section for gamma rays from group m to group n and from direction μ_o to μ is given by the equation

$$G_{m,n}(x,\mu,\mu_o) = \int_n dE \int_m dE_o\ G(x;\mu,E;\mu_o,E_o)f_m(E_o) \tag{4.16}$$

where $G(x;\mu,E;\mu_o,E_o)$ is the Klien-Nishina formula given by Equation 3.33.

The weighting function $f_m(E)$ has been selected to be of the form

$$f_m(E) = \text{constant} = \frac{1}{\Delta E_m} \tag{4.17}$$

where ΔE_m is the group width of group m. This form of the

weighting function assumes the energy dependence to be constant within the group.

The integration of the energy dependent equations with respect to the angular variable is approximated in the same manner as the monoenergetic equations using the shifted Gauss-Legendre quadrature formula.

$$\int_0^1 f(x)dx = \sum_{k=1}^{N} W_k f(x_k') \qquad (4.2)$$

Thus the reflections and transmission functions can be written in discrete form by letting

$$R_{m,n,i,j}(x) = r_{m,n}(x,\mu_i,\mu_j) \qquad (4.18)$$

$$T_{m,n,i,j}(x) = t_{m,n}(x;\mu_i,\mu_j) \qquad (4.19)$$

$$G_{m,n,i,j}(x) = G_{m,n}(x,\mu_i,\mu_j) \qquad (4.20)$$

where the subscripts m and n refer to the initial and final energy states respectively and the subscripts i and j refer to the discrete input angle and the discrete output angle respectively.

The equations in discrete form are

$$\frac{d}{dx} R_{m,n,i,j}(x) = G_{m,n,i,j}(x) - [\Sigma_m(x)/\mu_i + \Sigma_n(x)/\mu_j]$$

$$x \; R_{m,n,i,j}(x) + \sum_{k=1}^{M} \sum_{\ell=1}^{N} W_\ell G_{m,k,i,\ell}(x) R_{k,n,\ell,j}(x)/\mu_\ell$$

$$+ \sum_{k=1}^{M} \sum_{\ell=1}^{N} W_\ell R_{m,k,i,\ell}(x) G_{k,n,\ell,j}(x)/\mu_\ell$$

$$+ \sum_{k=1}^{M} \sum_{p=1}^{M} \sum_{\ell=1}^{N} \sum_{q=1}^{N} W_\ell W_q R_{m,p,i,q}(x) G_{p,k,q,\ell}(x)$$

$$x \; R_{k,n,\ell,j}(x)/\mu_\ell \mu_j \tag{4.21}$$

$$R_{m,n,i,j}(0) = 0 \tag{4.22}$$

and

$$\frac{d}{dx} T^s_{m,n,i,j}(x) = -[\Sigma_m(x)/\mu_i] T^s_{m,n,i,j}(x) + G_{m,n,i,j}(x) T^u_{n,j}(x)$$

$$+ \sum_{k=1}^{M} \sum_{\ell=1}^{N} W_\ell G_{m,k,i,\ell}(x) T^s_{k,n,\ell,j}(x)$$

$$+ \sum_{k=1}^{M} \sum_{\ell=1}^{N} W_\ell R_{m,k,i,\ell}(x) G_{k,n,\ell,j}(x) T^u_{,nj}(x)$$

$$+ \sum_{k=1}^{M} \sum_{p=1}^{M} \sum_{\ell=1}^{N} \sum_{q=1}^{N} W_\ell W_q R_{m,p,i,q}(x) G_{p,k,q,\ell}(x) T^s_{k,n,\ell,j}(x) \tag{4.23}$$

$$T^s_{m,n,i,j}(0) = 0 \tag{4.24}$$

$$T^u_{n,j}(x) = \exp[-1/\mu_j \sum_{r=1}^{R} \Sigma_n(x_r) \cdot x_r] \tag{4.25}$$

The subscripts m,n,k,p refer to energy groups while the subscripts i,j,ℓ,q refer to angular states. In all cases the first two subscripts of the reflection, transmission and

differential scattering cross section functions refer to the input and output energy groups while the second two subscripts refer to the input and output angles. The two subscripts of the unscattered flux refer to the final energy and angles states respectively. M is the number of energy groups and N is the number of angular groups. Thus the energy dependent integrodifferential equations have been replaced by a set of ordinary nonlinear differential equations. Compton scattering of gamma rays from a lower energy group to a higher energy group is not possible. If the energy groups are numbered from highest to lowest, then

$$R_{m,n,i,j}(x) = 0 \tag{4.26}$$

$$T_{m,n,i,j}(x) = 0 \tag{4.27}$$

for $n < m$. The size of the system for the reflection function is $N^2[M(M+1)/2]$. The size of the transmission function is $2N^2[M(M+1)/2]$ since the reflection function is also needed. Thus a three angle five energy group approximation would require 135 equations for the reflection function and 270 equations for the transmission function.

Differential Scattering Cross Section

$G_{m,n,i,j}(x)$ is determined from the Klein-Nishina differential cross section. It is given by

$$G_{m,n,i,j}(x) = \int_n dE \int_m dE_o G(x,\mu_j;E_i;\mu_i,E_o) f_m(E_o) \qquad (4.28)$$

where $f_m(E_o)$ is taken to be of the form

$$f_m(E_o) = \frac{1}{\Delta E_m} \qquad (4.29)$$

ΔE_m being the width of the group m.

When the variable E is changed to Compton wavelength λ, Equation 3.33 can be rewritten in the form

$$G_{m,n,i,j}(x) = n_e \frac{\lambda_m \lambda_{m-1}}{\lambda_m - \lambda_{m-1}} \int_n d\lambda \int_m d\lambda_o \, \sigma(\lambda,\mu_j;\lambda_o,\mu_i) \qquad (4.30)$$

where n_e is the electron density, λ_m is the wavelength corresponding to the energy at the lower limit of group m, and $\sigma(\lambda,\mu_j;\lambda_o,\mu_i)$ is the microscopic differential cross section for scattering. $\sigma(\lambda,\mu_j;\lambda_o,\mu_i)$ is given by the equation

$$\sigma(\lambda,\mu_j;\lambda_o,\mu_i) = \int_o^{2\pi} \sigma(0)\delta(\cos\theta - \lambda_o - 1 + \lambda)\, d\varphi \qquad (4.31)$$

$$= K(\lambda,\lambda_o) R_e [1/\pi \; 1 - \mu_i^2 - \mu_j^2 - \lambda^2 + 2\lambda\mu_i\mu_j] \qquad (4.32)$$

where

$$K(\lambda,\lambda_o) = \frac{3}{8} \frac{\lambda_o^2}{\lambda^2} \left[\frac{\lambda_o}{\lambda} + \frac{\lambda}{\lambda_o} + 2(\lambda_o - \lambda) + (\lambda_o - \lambda)^2\right] \qquad (4.33)$$

in Thompson units for $\lambda_o \leq \lambda \leq \lambda_o + 2$, $K(\lambda,\lambda_o) = 0$ for

all other λ_o and λ, and

$$\lambda = 1 + \lambda_o - \lambda \tag{4.34}$$

Integration of Equation 4.30 with respect to both λ and λ_o is performed by a five point Gauss-Legendre integration formula.

Calculation of Transmitted Flux

For dose calculations it is necessary to calculate the transmitted flux. The relation between the transmission function $T(x;\mu,E;\mu_o,E_o)$ and the transmitted flux for finite media $\varphi(x,E,\mu)$ is

$$\varphi(x,E,\mu) = T(x;\mu,E;\mu_o,E_o)J^o(x,\mu_o,E_o) \tag{4.35}$$

where $J^o(x,\mu_o,E_o)$ is the initial flux entering the slab. In discrete form Equation 4.35 becomes

$$\varphi_{n,j}(x) = T_{m,n,i,j}(x)J^o_{m,i}(x) \tag{4.36}$$

where the subscripts m and n refer to the initial and final energy groups and the subscripts i and j refer to the initial and final angular states. Thus the transmitted flux may be obtained for any type of source condition, with respect to angle and energy.

Using the notation described above the total transmitted flux in any energy group $\varphi_n(x)$ is

$$\varphi_n(x) = \sum_{j=1}^{N} W_j \varphi_{n,j}(x) \tag{4.37}$$

The total transmitted flux $\varphi(x)$ is given by

$$\varphi(x) = \sum_{n=1}^{M} \varphi_n(x)$$

$$= \sum_{n=1}^{M} \sum_{j=1}^{N} W_j T_{m,n,i,j}(x) J^{o}_{m,i}(k) \tag{4.38}$$

For the gamma dose calculations the total energy flux is more important than the total number flux. The energy flux $\varphi^E(x,E)$ is given by

$$\varphi^E(x,E) = E\varphi(x,E) \tag{4.39}$$

Using the energy group approximation the energy flux in a group n is

$$\varphi^E_n(x) = \int_n E\varphi(x,E)dE \tag{4.40}$$

The solution of Equation 4.40 is accomplished by first approximating the number flux by a polynomial of degree M-1 where M is the number of energy groups.

$$\varphi(x,E) = \sum_{i=o}^{M-1} a_i E^i \tag{4.41}$$

The number flux in each group then becomes

$$\varphi_n(x) = \int_n \varphi(x,E)dE = \int_n \sum_{i=0}^{M-1} a_i E^i dE$$

$$= \sum_{i=0}^{M-1} a_i [(E_u^{i+1} - E_L^{i+1})_n/i+1] \qquad (4.42)$$

$$n=1,2,3,\ldots M$$

where E_n and E_L are the upper and lower energies of group n respectively. The set of equations (4.42) can be solved for the coefficients a_i. The energy flux is then found by solving the set of equations

$$\varphi_n^E(x) = \int_n E\varphi(x,E)dE = \int_n \Sigma a_i E^{i+1}$$

$$= \Sigma a_i [(E_u^{i+2} - E_L^{i+2})_n/i+2] \qquad (4.43)$$

$$n = 1,2,3,\ldots M$$

Energy Buildup Factor

The energy buildup factor is defined by the ratio of the actual transmitted energy flux φ_{out}^E to the initial energy flux times the exponential attenuation.

$$B_E = \varphi_{out}^E/\varphi_{in}^E \exp[-\Sigma(x)x]$$

For gamma dose calculations the energy buildup factor is calculated from the relation

$$B_E = \frac{\sum_{i=1}^{M} [\varphi_i^E + \bar{E}_i \varphi_i^u]}{\sum_{i=1}^{M} \bar{E}_i \varphi_i^u} \qquad (4.44)$$

where $\bar{E}_i$ is the average energy of the incident group i and φ_i^u is the uncollided number flux in the ith group. For the monoenergetic case this reduces to

$$B_E = \frac{\sum_{i=1}^{M} \varphi_i^E + \bar{E}_1 \varphi_1^u}{\bar{E}_1 \varphi_1^u} \tag{4.45}$$

Numerical Integration Method

A wide variety of numerical methods are available for the solution of sets of ordinary nonlinear differential equations. Because the number of equations for the solution of the reflection and transmission functions 4.21 and 4.23 is quite large it is advantageous to use the fastest possible numerical method that will yield the desired accuracy. It is also advantageous to use a numerical method which furnishes some criterion for determining whether or not the step size should be changed at any given point in the solution. The derivatives of both the reflection and the transmission functions change rapidly for small values of x but change much less rapidly for values of a greater that one mean free path. This means small step sizes must be taken for small values of x but larger step sizes can be taken for x greater than one mean free path.

The predictor-corrector methods are well suited for the solution of the reflection and transmission functions and have several advantages relative to the more common methods

such as Runge-Kutta methods.

1. The predictor-corrector methods require fewer evaluations of the derivative at each step in the solution. This can substantially reduce the computation time.

2. The truncation error is easier to estimate since its form is simpler than that for the Runge-Kutta method.

3. The absolute value of the difference between the predicted and corrected values at a particular step in the predictor-corrector methods furnishes a criterion for determining whether the integration interval should be lengthened, shortened or left unchanged. This criterion is not available in the Runge-Kutta method.

The predictor-corrector methods have at least two disadvantages:

1. They are not self starting and thus require starting points calculated by some other method.

2. The solution produced by the predictor-corrector method can become unstable and oscillate with increasing-magnitude for some differential equations.

The possible instability problem is the only serious disadvantage of the method.

Those who report numerical results for the solution of the reflection and transmission functions have used the Runge-Kutta method most often. Bellman reports detailed calculations using the Runge-Kutta method for the reflection of light in stellar atmospheres. Mathews evaluated the

Runge-Kutta method, the Adams predictor-corrector method and several approximations based on exponentials for the problem of neutron transport. He found the Runge-Kutta method easy to apply but very slow. The Adams method was much faster but was discarded because of instability problems. The exponential approximations proved best for his problem; however, this method also developed instabilities for large step sizes.

The previous computational work indicates that most common methods for solution of ordinary nonlinear differential equations do not work well when applied to the invariant imbedding equations, the Runge-Kutta method because it is relatively slow and common predictor-corrector methods because of instability problems.

R. L. Crane has developed a modified predictor-corrector method having a significantly larger range of stability. His method was used throughout this thesis to solve the invariant imbedding equations. No stability problems were encountered in the applications presented in this thesis. This is shown in detail in Chapter Five. The Crane predictor-corrector procedure is given by:

A. predictor equation

$$P_{n+1} = a_3 y_n + a_2 y_{n-1} + a_1 y_{n-2} + a_0 y_{n-3}$$
$$+ h(b_3 y'_n + b_2 y'_{n-1} + b_1 y'_{n-2} + b_0 y'_{n-3}) \qquad (4.46)$$

B. corrector equation

$$c_{n+1} = f_3 y_n + h(d_4 P_{n+1} + d_3 y'_n + d_2 y'_{n+1} + d_1 y'_{n-2}) \qquad (4.47)$$

where

$a_3 = 1.5476511$

$a_2 = -1.8675052$

$a_1 = 2.0172069$

$a_o = -0.69735280$

$b_3 = 2.0022472166667$

$b_2 = -2.03168765$

$b_1 = 1.81861065$

$b_o = -0.1143200166667$

$f_2 = 1.0$

$d_4 = 0.375000$

$d_3 = 0.79166607$

$d_2 = -0.208333333$

$d_1 = 0.04166666667$

and where h is the step size.

The starting points are obtained by the Runge-Kutta-Gill procedure given by

$$y_{n+1} = y_n + \frac{1}{6}\,(k_1 + 2(1-\sqrt{\tfrac{1}{2}})k_2 + 2(1+\sqrt{\tfrac{1}{2}})k_3 + k_4 \qquad (4.48)$$

where

$k_1 = hf(x_n, y_n)$

$k_2 = hf(x_n + \frac{1}{2}h, y_n + \frac{1}{2}k_1)$

$$k_3 = hf(x_n+\tfrac{1}{2}h,\ y_n+(-\tfrac{1}{2}+\sqrt{\tfrac{1}{2}})k_2 +(1-\sqrt{\tfrac{1}{2}})k_2)$$

$$k_4 = hf(x_n+h, g_n-\sqrt{\tfrac{1}{2}}\ k_2 + (1+\sqrt{\tfrac{1}{2}})k_3)$$

Crane's predictor-corrector method along with the Runge-Kutta-Gill starting procedure has been incorporated into a subroutine package called NODE by the Iowa State University computation center. This subroutine package was used in the computer code developed for solving the transmission and reflection equations. In NODE the relative error at each point is approximated by

$$E = \left|\frac{P_{n+1}-C_{n+1}}{C_{n-1}}\right| \tag{4.49}$$

where P_{n+1} is the predicted value and C_{n+1} is the corrected value. The step size of the integration is automatically changed depending on the size of the error estimates. The step size is halved if E_{max}, the largest value of E at any given step, is greater than 16.219658×10^{-T} where T is an integer value read into the program. The step size is doubled if for three consecutive steps E_{max} is less than $16.219658/200 \times 10^{T}$.

Computer Code

A flow diagram of the computer code is shown in Figure 4. The actual solution of the invariant imbedding equations is obtained from the NODE subroutine. The main program is used to input the necessary parameters for the solution and

Figure 4. Flow diagram of computer program

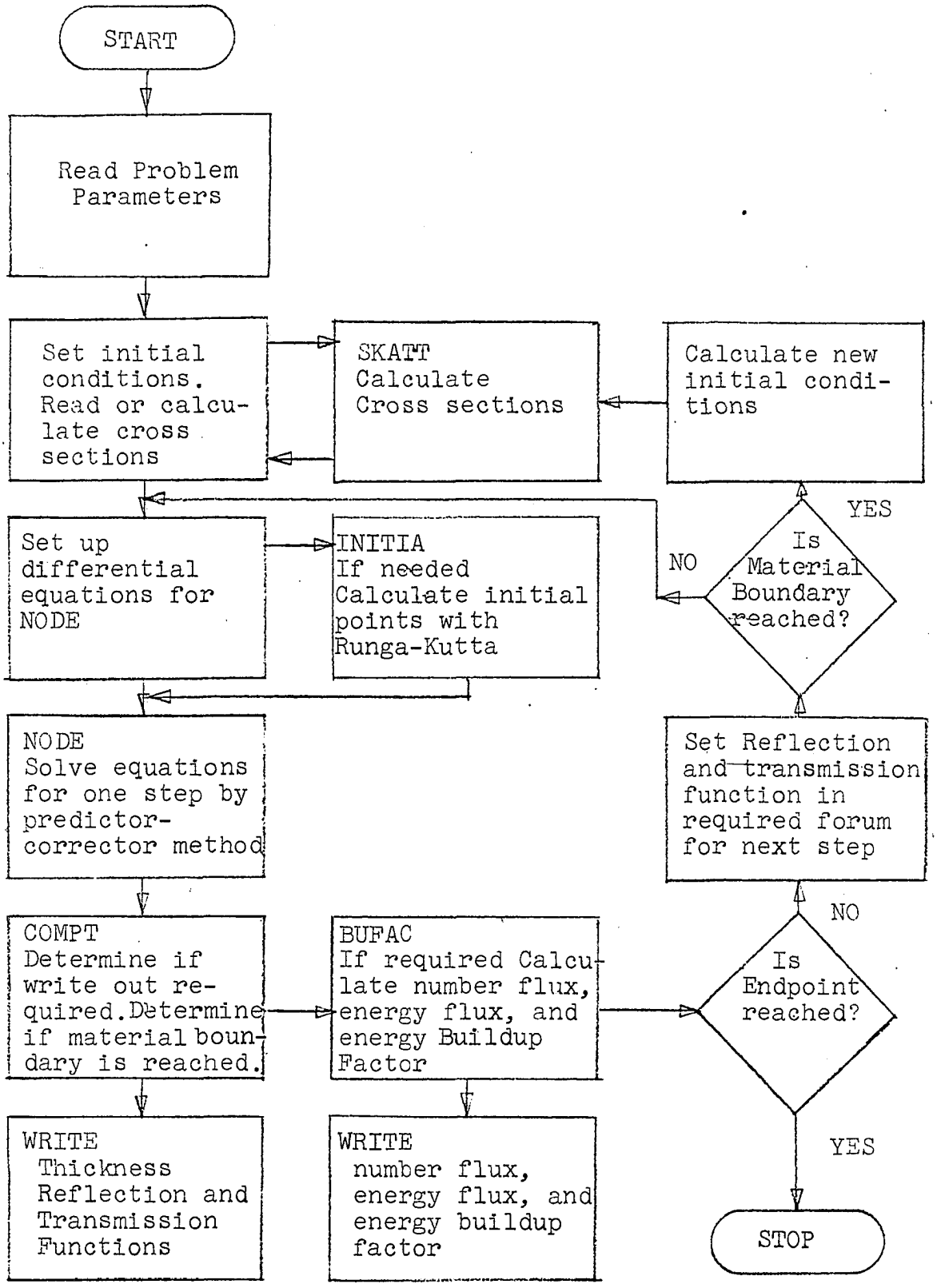
START
Read Problem Parameters
Set initial conditions. Read or calculate cross sections
SKATT Calculate Cross sections
Calculate new initial conditions
Set up differential equations for NODE
INITIA If needed Calculate initial points with Runga-Kutta
Is Material Boundary reached?
YES
NO
NODE Solve equations for one step by predictor-corrector method
Set Reflection and transmission function in required forum for next step
COMPT Determine if write out required. Determine if material boundary is reached.
BUFAC If required Calculate number flux, energy flux, and energy Buildup Factor
Is Endpoint reached?
NO
YES
WRITE Thickness Reflection and Transmission Functions
WRITE number flux, energy flux, and energy buildup factor
STOP

to specify the type of output wanted. The subroutine COMPY was used to put the invariant imbedding equations in the form required for NODE. The initial values for the predictor-corrector procedure are calculated in the subroutine INITIA. The calculated reflection and transmission functions are written out or punched on cards according to the specifications of the problem in subroutine COMPT. The number flux, energy flux and energy buildup factor are calculated in subroutine BUFAC. For gamma dose calculations the program was developed so that the scattering cross sections and total attenuation cross sections could be either calculated in subroutine SKATT or read in on cards. The initial flux is read in on cards. This flux can be of any type with respect to angle and energy. For multilayered slabs the initial flux is calculated from the transmission function at each material boundary, and the problem restarted.

CHAPTER FIVE. APPLICATIONS

Introduction

Although the main objective of this thesis was to develop numerical and computational techniques for the gamma transport problem, two other problems were studied in detail. The problem of light transport in stellar atmospheres was studied because of the large amount of data available for comparison. These data are due mainly to Bellman (3). The wealth of data provides an excellent check on the numerical methods used to solve the reflection and transmission functions. These data also provide a means to test the range and limits of accuracy of the approximations made to the rigorous theory. The critical size problem is studied because direct comparisons can be made between Carlson's S_N method and the invariant imbedding method.

Computational methods have been developed to find the number flux, energy flux and energy buildup factor for the gamma transport problem. Further approximations have been made to the discrete equations to shorten computer time. The calculated energy buildup factor and differential energy spectrum for various materials were then compared to moments method calculations.

Radiative Transport in Stellar Atmospheres

The particular physical model used in this study is identical to the models used by Ambarzumian (1), Chandrasekhar (16), and Bellman (3). It is assumed that parallel rays of light of uniform intensity are incident upon a slab composed of material that absorbs and scatters light. It is desired to determine the intensity of the diffusely reflected and diffusely transmitted light as a function of the intensity of the incident flux, composition of the slab, and angles of incidence, reflection and transmission. The properties of the medium composing the slab are the following:

1. In traversing a distance x in any direction in the slab the intensity I of the light is reduced by absorption to $Ie^{-\sigma x}$.

2. A fraction λ of the absorbed light is reradiated and the remaining fraction $1-\lambda$ is lost. In this context λ is called the albedo for single scattering.

3. Radiation is scattered isotropically without changing polarization.

4. Following the techniques of Ambarzumian, Chandrasekhar and Bellman, both the scattering albedo λ and the scattering cross section σ are assumed to be constant throughout the medium.

The reflection and transmission functions for this problem are defined as follows:

$r(x,\mu,\mu_o)$ is the specific intensity of reflected light in the direction θ per unit area on the face of a slab of thickness x due to a beam of unit intensity incident at angle θ_o.

$t(x,\mu,\mu_o)$ is the specific intensity of light per unit area in the direction θ transmitted through a slab of thickness x due to a beam of unit intensity incident at angle θ_o.

The reflection and transmission functions for this problem are given by Equations 3.47 and 3.48 respectively. The discrete forms of these equations are given by Equations 4.6 and 4.8.

Typical reflection functions

The computational results for this problem are shown in Figures 5 through 8 for albedoes of 0.5 and 0.9, for angles of incidence of 60^o and 13^o, and for several values of the thickness of the slab. The results are shown for both five and seven discrete angular approximations. As can be seen from the figures, the N = 5 and N = 6 calculations agree very well.

Comparison with Ambarzumian's results

Ambarzumian (1) tabulates values of a function $\varphi(n)$ in terms of which it is possible to express the intensity of the light diffusively reflected from a homogeneous slab of

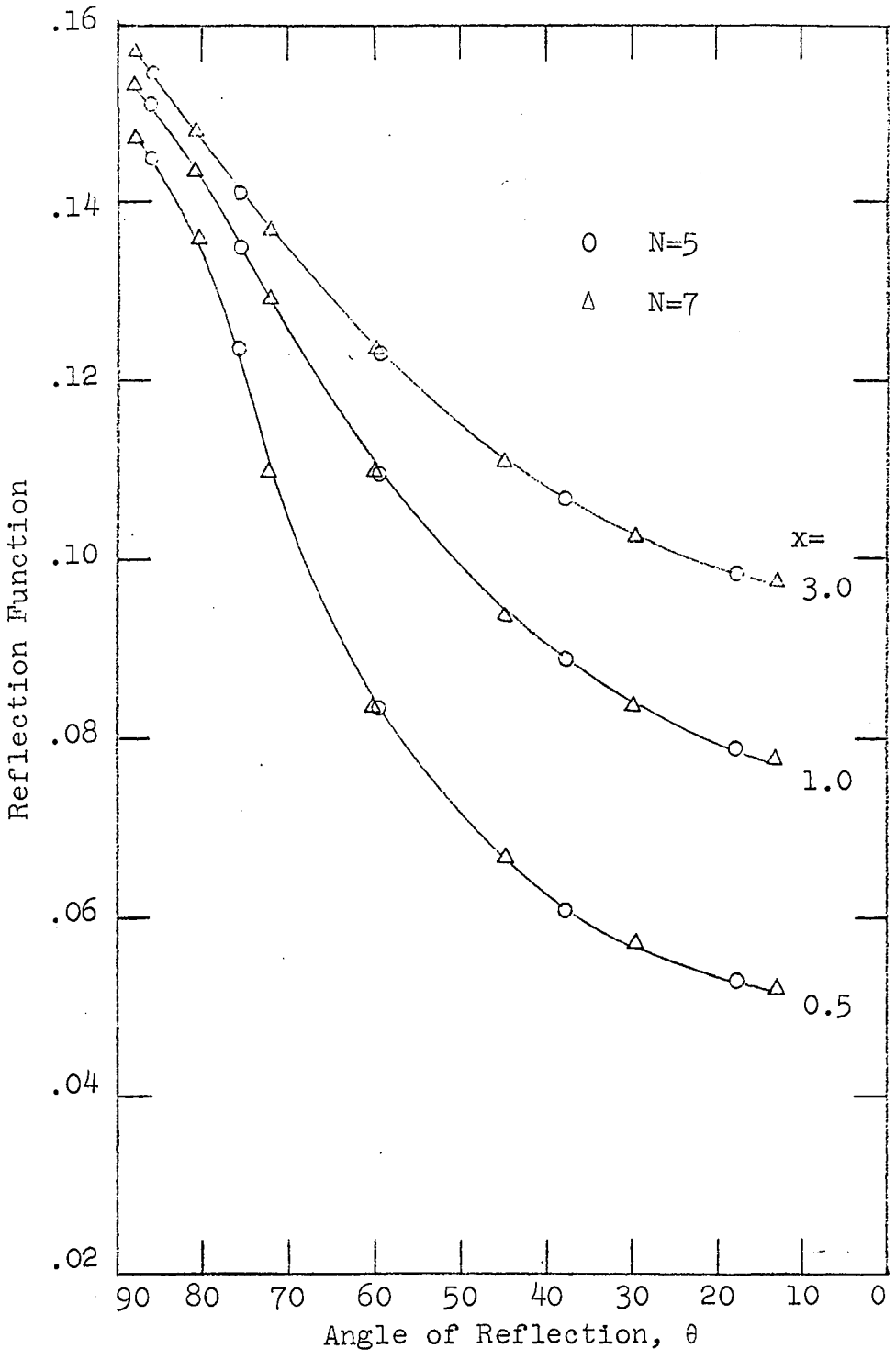

Figure 5. Reflection function for incidence angle of 60° and albedo of 0.5

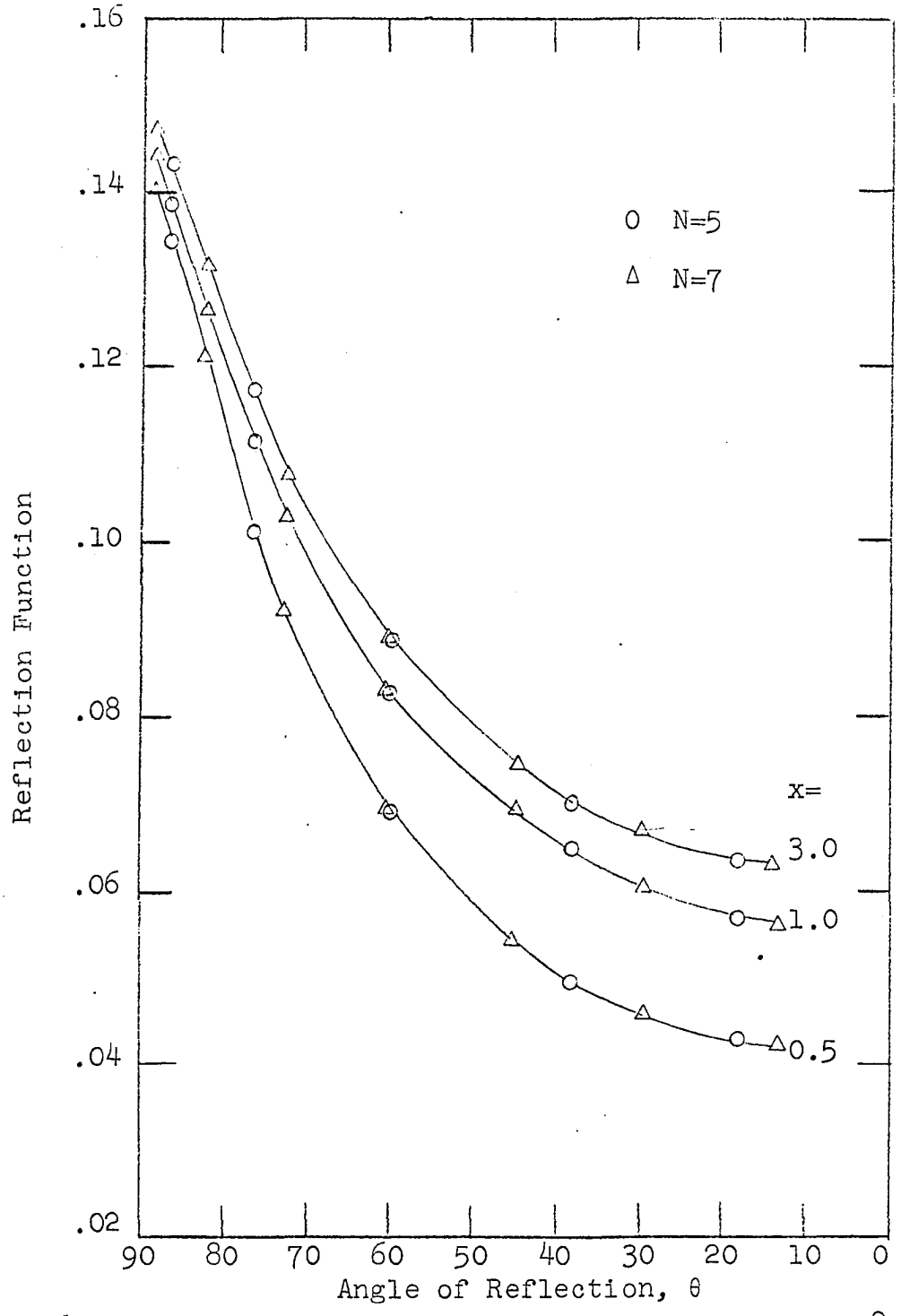

Figure 6. Reflection function for incidence angle of 13° and albedo of 0.5

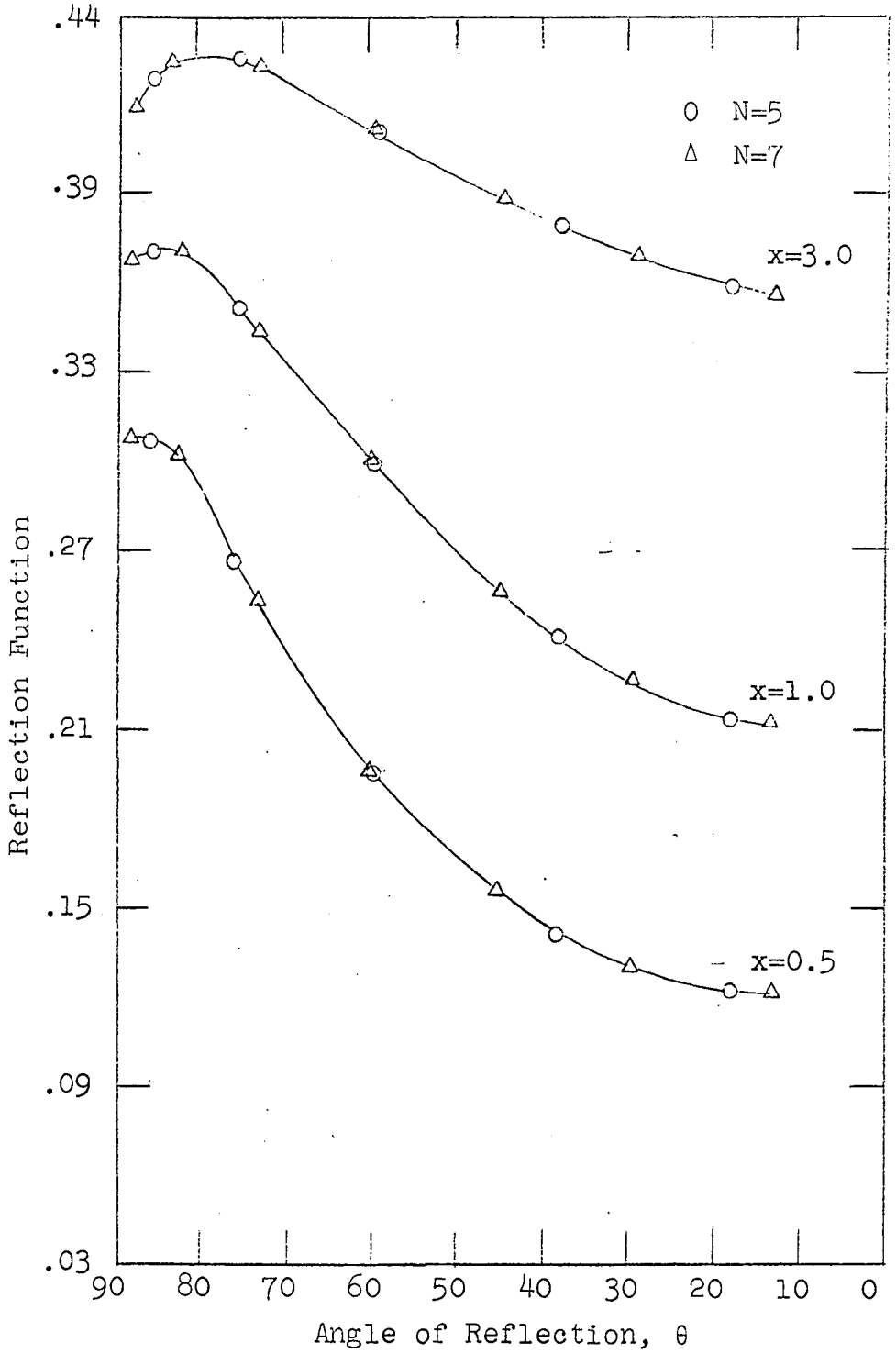

Figure 7. Reflection function for incidence angle of 13° and albedo of 0.9

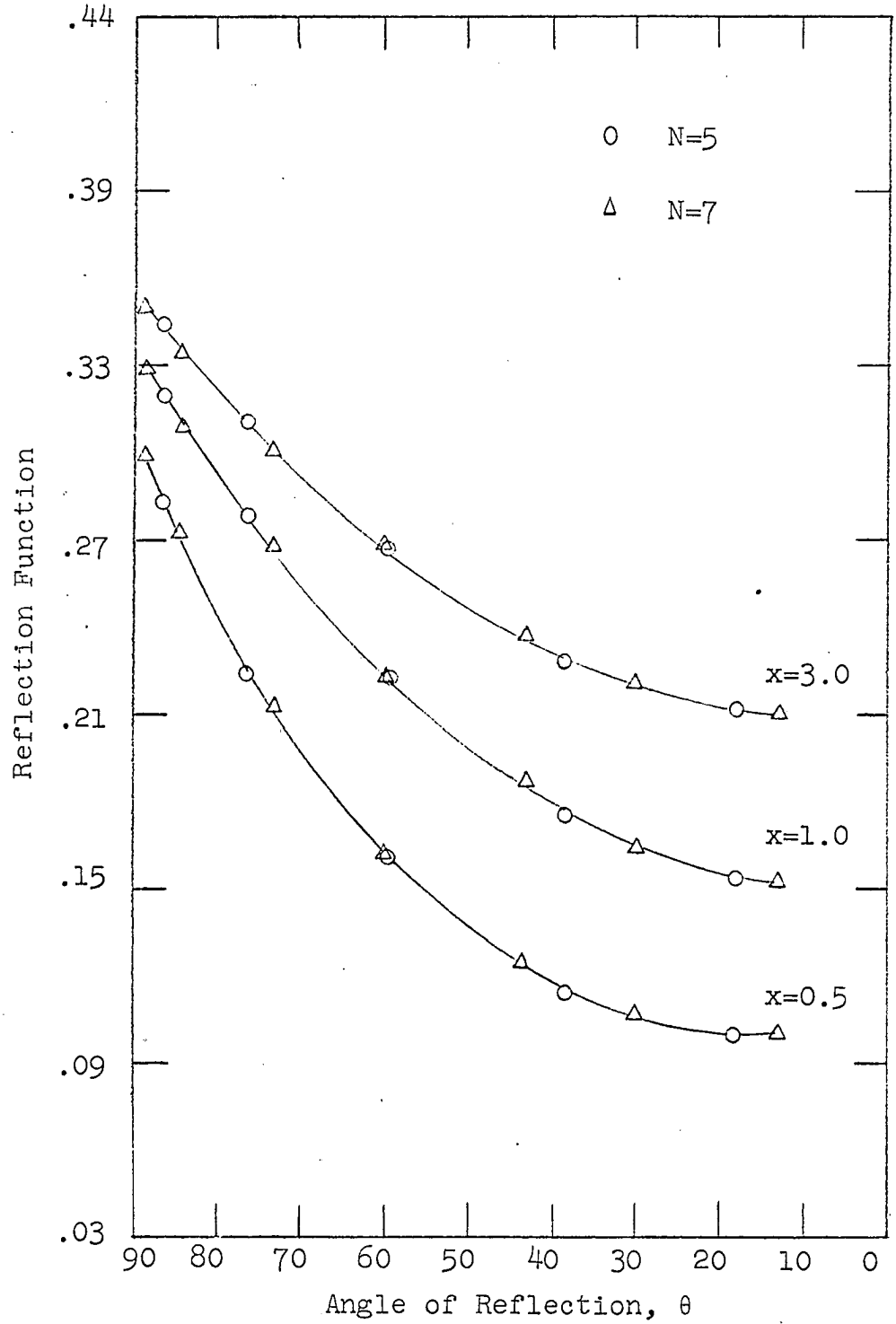

Figure 8. Reflection function for incidence angle of 60° and albedo of 0.9

infinite thickness. These values can be used to determine the limiting values of the reflection function approached by slabs of increasing thickness. It was found that for $\lambda \leq 0.5$ at a thickness of 3.0 mean free paths the values of reflection function remained constant. This thickness was considered essentially equivalent to an infinite thickness. For example, when $\lambda = 0.5$ and the thickness of the slab is 3.0 mean free paths, the calculated value of the reflection function is 0.0969. For the slab of infinite thickness under the same conditions, Ambarzumian's value for the reflection function is 0.0976. For smaller values of λ the agreement is even better. It was necessary to go to thicknesses of 6.0 mean free paths before the reflection functions became constant for $\lambda = 0.6$ to 0.9. There is still good agreement with Ambarzumian's values for the infinite slab. For $\lambda = 0.9$ and the same angles as above the calculated value of $r(v,u,x)$ at $x = 6.0$ is 0.379. Ambarzumian's table yields 0.381 for the infinite slab.

Comparison with Bellman's results

Bellman (3) has calculated the reflection function using Runge-Kutta integration scheme with seven discrete angles ($N = 7$) and with albedos from 0.1 to 1.0 over thicknesses from 0.1 to 6.0 mean free paths. The results found using Crane's predictor-corrector method agree with Bellman's

results for seven discrete angles to within 0.5% over all ranges of λ and x. In addition to direct comparison with Bellmen's work, studies were made to determine the accuracy of the angular approximations for various albedos. Comparison was made with Bellman's calculations for N = 2, 3, 5, 7 with albedos from 0.1 to 0.9. The results obtained for N = 5, 7 agree to within 0.5%. Excellent agreement was also found for N = 2 and 3 if the albedo was small, however, large discrepancies developed for albedos greater than 0.6. Figures 9 and 10 show the results of these studies for albedos of 0.2 and 0.9. The contribution to the reflection at 60° is plotted against the incidence angle in these figures.

Comparison with Chandrasekhar's results

In his book Radiative Transfer (16) Chandrasekhar solves the invariant imbedding equations for slabs of finite thickness. He illustrates the solutions for the reflection function for λ = 0.9 and 1.0 based on rational approximations to the X and Y functions. Very good agreements is found with his values, particularly for small thicknesses. Chandrasekhar also tabulates values for the transmission function based on the same approximations. His results and the calculates values of the transmission functions for N = 5 are shown in Figure 11.

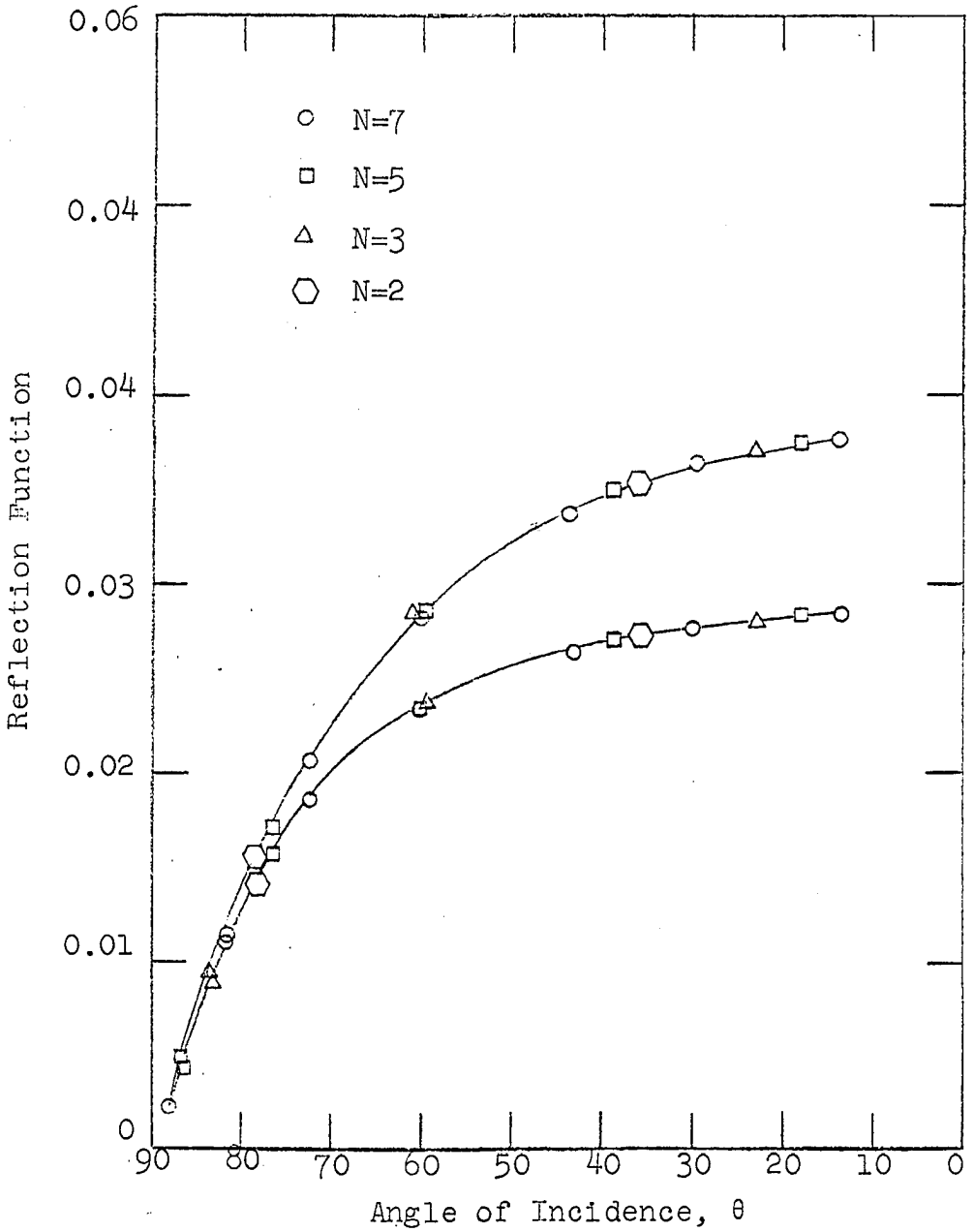

Figure 9. Reflection function for incidence angle of 60° and albedo of 0.2

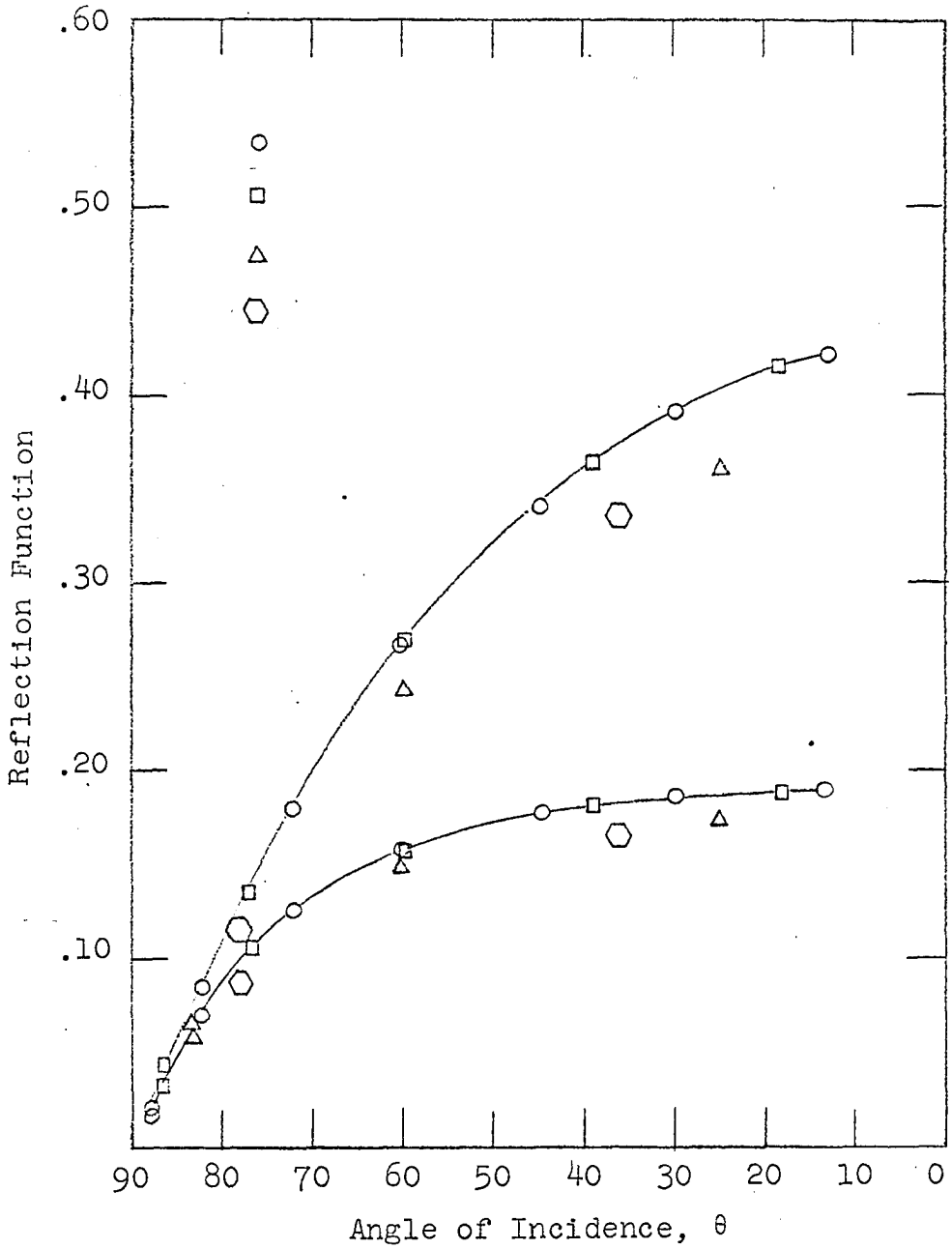

Figure 10. Reflection function for incidence angle of 60° and albedo of 0.9

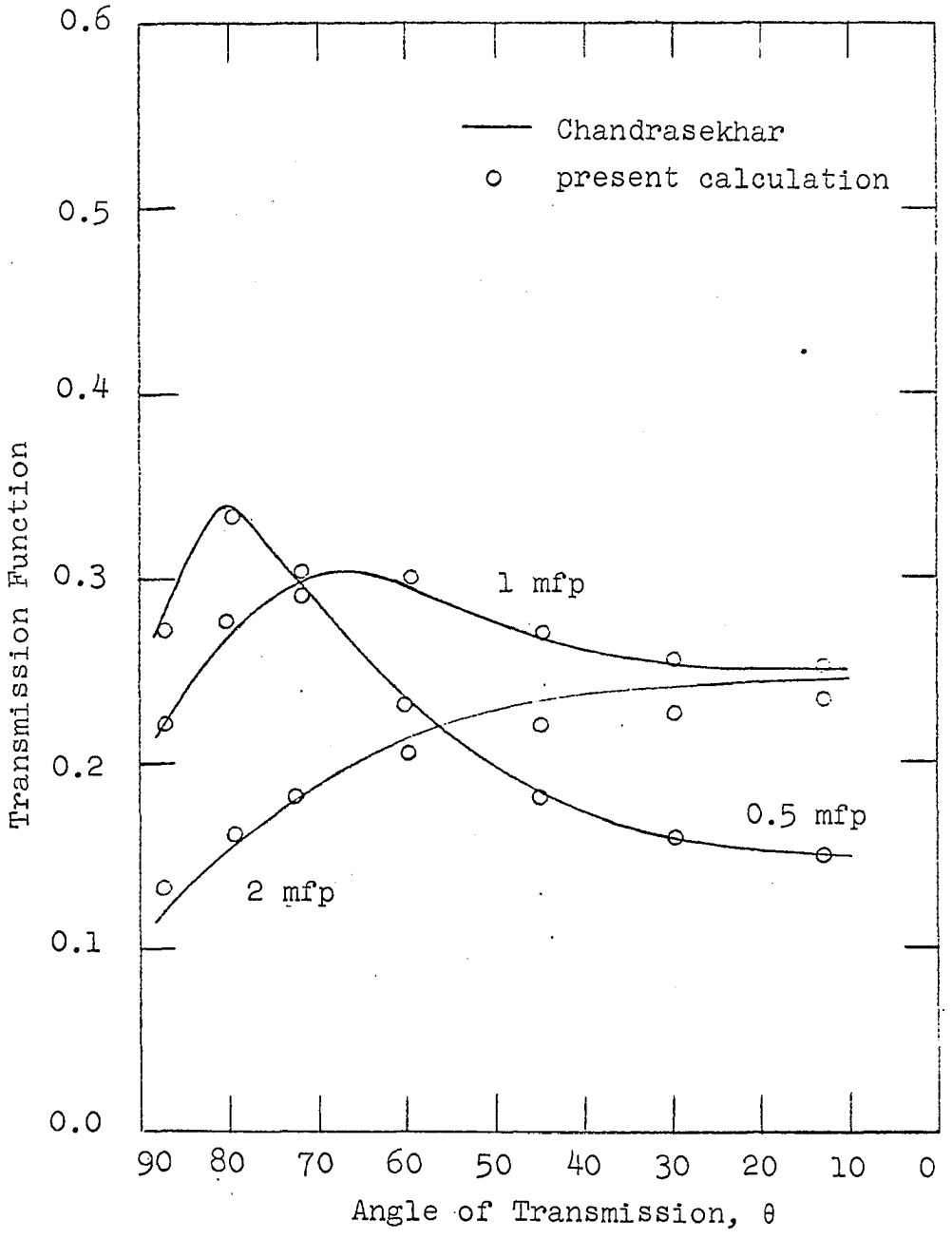

Figure 11. Transmission function for incidence angle of 60° and albedo of 0.6

Numerical stability of predictor-corrector method

Because of the possibility of numerical instability when using predictor-corrector methods, the numerical results for the reflection and transmission functions were checked for any oscillatory behavior of the solutions from step to step. In all cases there was no indication that the solution was oscillating. This coupled with the fact that the present calculations agree with the calculations obtained by other methods indicates Crane's predictor-corrector method is numerically stable when used to solve the monoenergetic reflection and transmission equations. The advantage of the method is shown in Table 1 where the step size and results for the reflection function with $\lambda = 0.5$ is compared to Bellman's results using the Runge Kutta method with a fixed step size of 0.01.

Table 1. Reflection function for $\lambda = 0.5$

Distance m.f.p.	Present Calculation Step size m.f.p.	$R(x,\mu,\mu_o)$ $\mu=\mu_o=60^o$	Bellman $R(x,\mu,\mu_o)$ $\mu=\mu_o=60^o$ Step Size=0.01
0	0.015625	0.0	0.0
0.2	0.031250	0.039568	0.039504
0.4	0.062500	0.061652	0.061629
1.5	0.062500	0.087099	0.087096
2.0	0.125000	0.087900	0.087888
3.0	0.062500	0.088110	0.088107

Critical Size Problem

The critical size problem presented here is the same as described by Carlson (15) at the Second International Conference on the Peaceful Uses of Atomic Energy. As the mean number of secondary neutrons per collision increases the critical size of a bare homogeneous slab decreases to the point where edge effects become increasingly important. Diffusion theory fails at this point and the accuracy of the approximation to the transport theory can be tested. Carlson reports the critical thickness values for various orders of approximation and for the number of secondaries per collision up to C = 2.

The critical size problem using invariant imbedding theory has the straightforward theoretical condition that the reflection and transmission functions become infinite at the critical thickness

$$r(x_c, \mu, \mu_o) = \infty$$

$$t(x_c, \mu, \mu_o) = \infty$$

where x_c refers to the critical thickness.

The case in which the mean number of secondaries per collision equals 2.0 was chosen for study. The invariant imbedding calculations for N = 2, 3, 5, 7 are compared to Carlson's (15) results for the S_N calculation using N = 2, 4, 8, 16 in Table 2. The general nature of the reflection function as the critical thickness is approached is shown in

Figure 12.

The results of this study show the high order of accuracy that is obtained using invariant imbedding techniques. The results also indicate that the N = 5 approximation is as good as the N = 7 approximation in this particular problem.

Table 2. Critical size of a bare multiplying slab

Invariant Imbedding c=2		S_N Method c=2	
Order of Calculations N	Critical Thickness x_c(mfp)	Order of Calculations N	Critical Thickness x_c(mfp)
2	0.51683	2	0.8194
3	0.59315	4	0.6526
5	0.62198	8	0.6274
7	0.62194	16	0.6232

Gamma Transport Problem

The objectives of the gamma transport problem are the calculation of the transmitted energy flux, the differential energy spectrum and the energy buildup factor for finite media. The transmitted energy flux can be calculated from the energy dependent transmission function using the set of Equations 4.43. The differential energy spectrum can then be plotted from these data. The energy buildup factor then can be calculated from Equation 4.45.

Figure 12. Reflection function for a bare multiplying slab

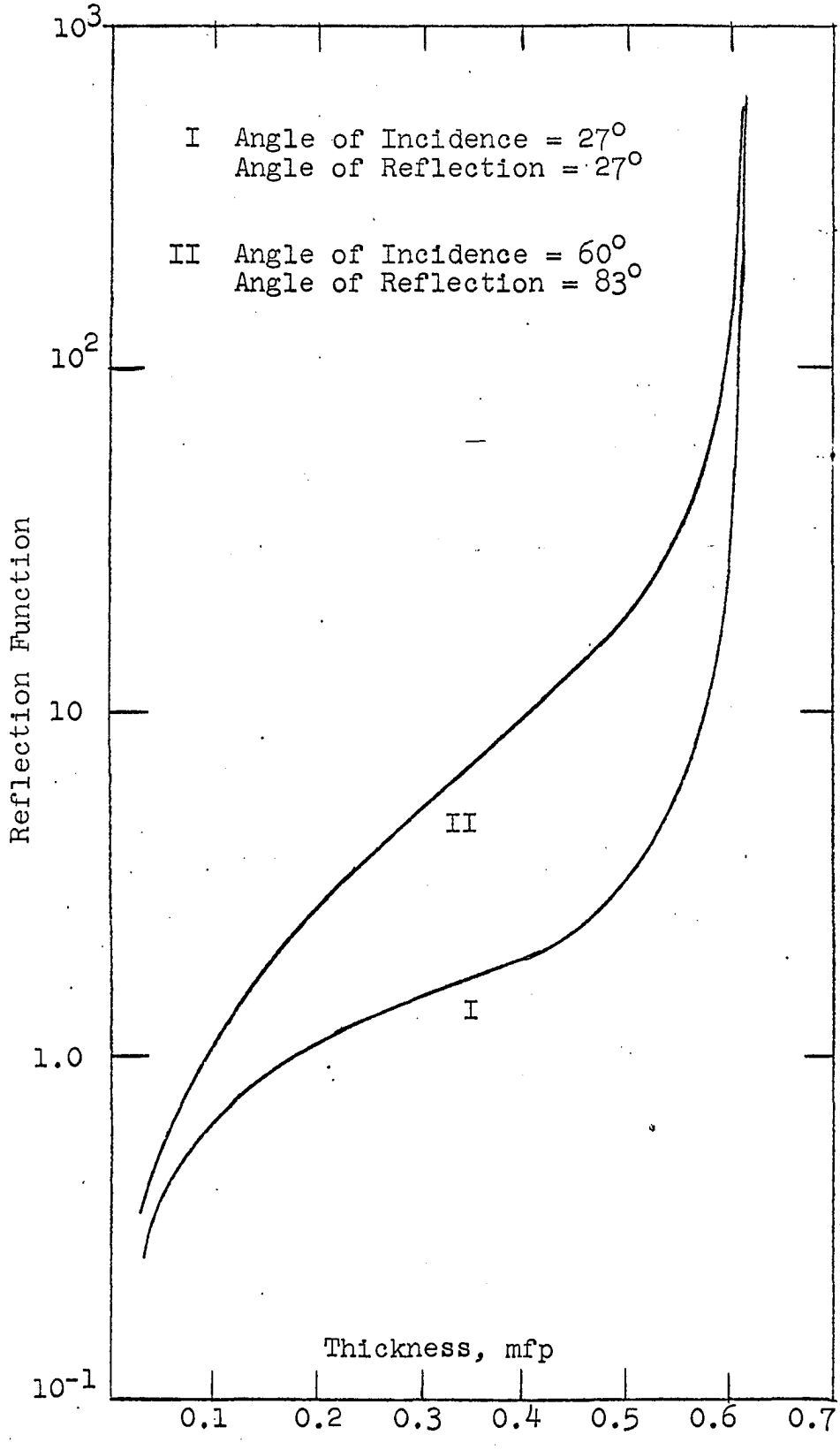
I Angle of Incidence = 27°
Angle of Reflection = 27°
II Angle of Incidence = 60°
Angle of Reflection = 83°
Reflection Function
10³
10²
10
1.0
10⁻¹
II
I
Thickness, mfp
0.1
0.2
0.3
0.4
0.5
0.6
0.7

The energy dependent transmission function is described by Equations 3.26 and 3.29. These equations in discrete form are given by

$$\frac{d}{dx} T^{s}_{m,n,i,j}(x) = -[\Sigma_m(x)/\mu_i]T^{s}_{m,n,i,j}(x)+G_{m,n,i,j}(x)T^{u}_{n,j}(x)$$

$$+\sum_{k=1}^{M}\sum_{\ell=1}^{N} W_e G_{m,n,i,\ell}(x)T^{5}_{k,n,\ell,j}(x)$$

$$+\sum_{k=1}^{M}\sum_{\ell=1}^{N} W_e R_{m,k,i,\ell}(x)G_{k,n,\ell,j}(x)T^{u}_{n,j}(x)$$

$$+\sum_{k=1}^{M}\sum_{p=1}^{M}\sum_{\ell=1}^{N}\sum_{q=1}^{N} W_e W_q R_{m,p,i,q}(x)G_{p,k,q,\ell}(x)$$

$$x \quad T^{s}_{k,n,\ell,j}(x) \tag{4.23}$$

$$T^{u}_{n,j}(x) = \exp[-1/\mu_j \sum_{r=1}^{R} \Sigma_n(x_r)\cdot x_r] \tag{4.26}$$

The transmission equations contain terms requiring the reflection function. Thus to solve Equations 4.23 and 4.26 the reflection function must first be calculated from Equation 4.21. The total number of equations which must be solved is $N^2M(M+1)$.

It was found that not all terms of Equation 4.23 contributed significantly to the transmission function. The terms containing the reflection function were found to be at least two orders of magnitude smaller than the other terms. If the terms of Equation 4.23 are defined by

$$A_1 = -[\Sigma_m(x)/\mu_1]T^s_{m,n,i,j}(x)$$

$$A_2 = G_{m,n,i,j}(x)T^u_{n,j}(x)$$

$$A_3 = \sum_{k=1}^{M}\sum_{\ell=1}^{N} W_e\, G_{m,n,i,\ell}(x)T^s_{k,n,\ell,j}(x)$$

$$A_4 = \sum_{k=1}^{M}\sum_{\ell=1}^{N} W_e R_{m,k,i,\ell}G_{k,n,\ell,j}(x)T^u_{n,j}(x)$$

$$A_5 = \sum_{k=1}^{M}\sum_{p=1}^{M}\sum_{\ell=1}^{N}\sum_{q=1}^{N} W_e W_q R_{m,p,i,q}(x)G_{p,k,q,\ell}(x)$$

$$\times\ T^s_{k,n,\ell,j}(x)$$

then the contribution of these terms to the transmission function at several mean free paths of lead is shown in Table 3. A 2-MEV monoenergetic source was used in this calculation.

The difference in magnitude of the five terms of Equation 4.23 can be explained from an examination of the physical processes involved. The terms involving the reflection function require the photon to be backscattered twice before passing through the slab. This is represented geometrically by term T_3 in Figure 3. The contribution to the energy flux of this photon is very small.

Since the terms containing the reflection function did not contribute significantly to the transmission function they were dropped. In this form the transmission function becomes

Table 3. Contributions to the transmitted energy flux in lead due to a 2 MEV source

Thickness mfp	Unscattered Energy Flux	Scattered Energy Flux	A_1	A_2	A_3	A_4	A_5
1	0.28844	0.18310	0.12961	-0.7326	0.12715	0.00042	0.00018
2	0.07521	0.06548	0.03316	-0.02588	0.06660	0.00022	0.00011
3	0.021909	0.02464	0.00867	-0.00711	0.02295	0.00008	0.00005
4	0.00588	0.00804	0.00232	-0.00101	0.00905	0.00004	0.00002
5	0.00171	0.00278	0.00061	-0.00059	0.00334	0.00002	0.00001

$$\frac{d}{dx} T^{s}_{m,n,i,j}(x) = -[\Sigma_m(x)/\mu_i]T^{s}_{m,n,i,j}(x)$$

$$+G_{m,n,i,j}(x)T^{u}_{n,j}(x) + \sum_{k=1}^{M}\sum_{\ell=1}^{N} W_e G_{m,n,i,\ell}(x)$$

$$x \quad T^{s}_{k,n,\ell,j}(x)$$

and

$$T^{u}_{n,j}(x) = \exp[-1/\mu_j \sum_{r=1}^{R} \Sigma_n(x_r)\cdot x_r] \qquad (5.1)$$

Using the set of Equations 5.1 the number of equations required is reduced by half. Also the calculation of the derivatives at each step in the solution is simplified. The result of this approximation is a significant decrease in the calculation time without a serious loss of accuracy.

Differential energy spectrums

The differential energy spectrums for photons transmitted through lead, uranium and water are shown in Figures 13 through 17. The transmitted energy flux, normalized by the unscattered portion of the transmitted energy flux, is plotted against energy in these figures. The transmitted energy flux was calculated using the set of Equations 5.1. A two discrete angle, five energy group approximation was used for all these calculations. The differential energy spectrum calculated by the moments method is also shown in Figures 13 through 17 for comparison. The differential energy spectrums calculated using Equation 5.1 agree very

Figure 13. Differential energy spectrum for 2 MEV gamma rays transmitted through four mean free paths of load

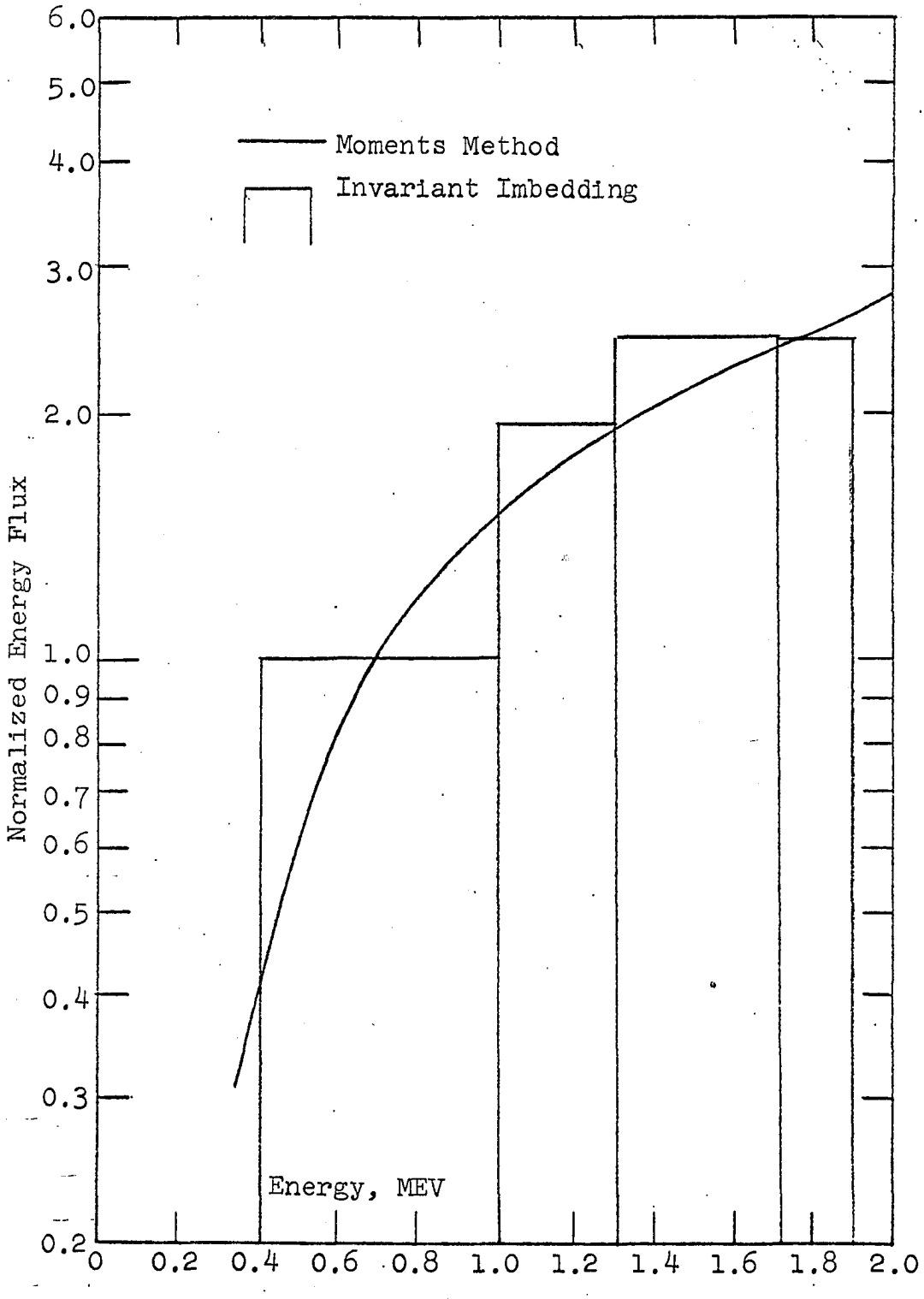
Moments Method
Invariant Imbedding
Normalized Energy Flux
Energy, MEV
6.0
5.0
4.0
3.0
2.0
1.0
0.9
0.8
0.7
0.6
0.5
0.4
0.3
0.2
0
0.2
0.4
0.6
0.8
1.0
1.2
1.4
1.6
1.8
2.0

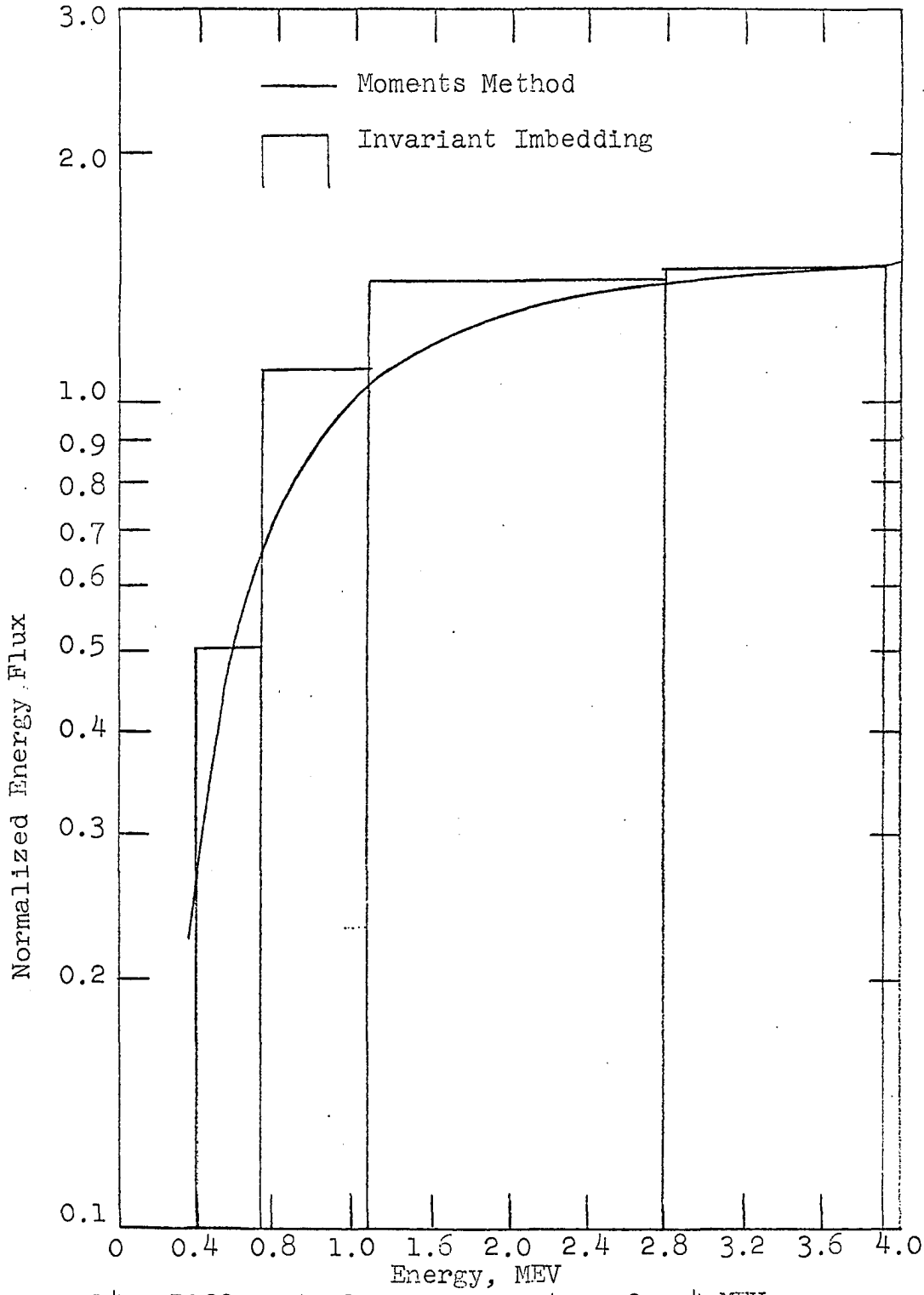

Figure 14. Differential energy spectrum for 4 MEV gamma rays transmitted through four mean free paths of lead

Figure 15. Differential energy spectrum for two MEV gamma rays transmitted through four mean free paths of uranium

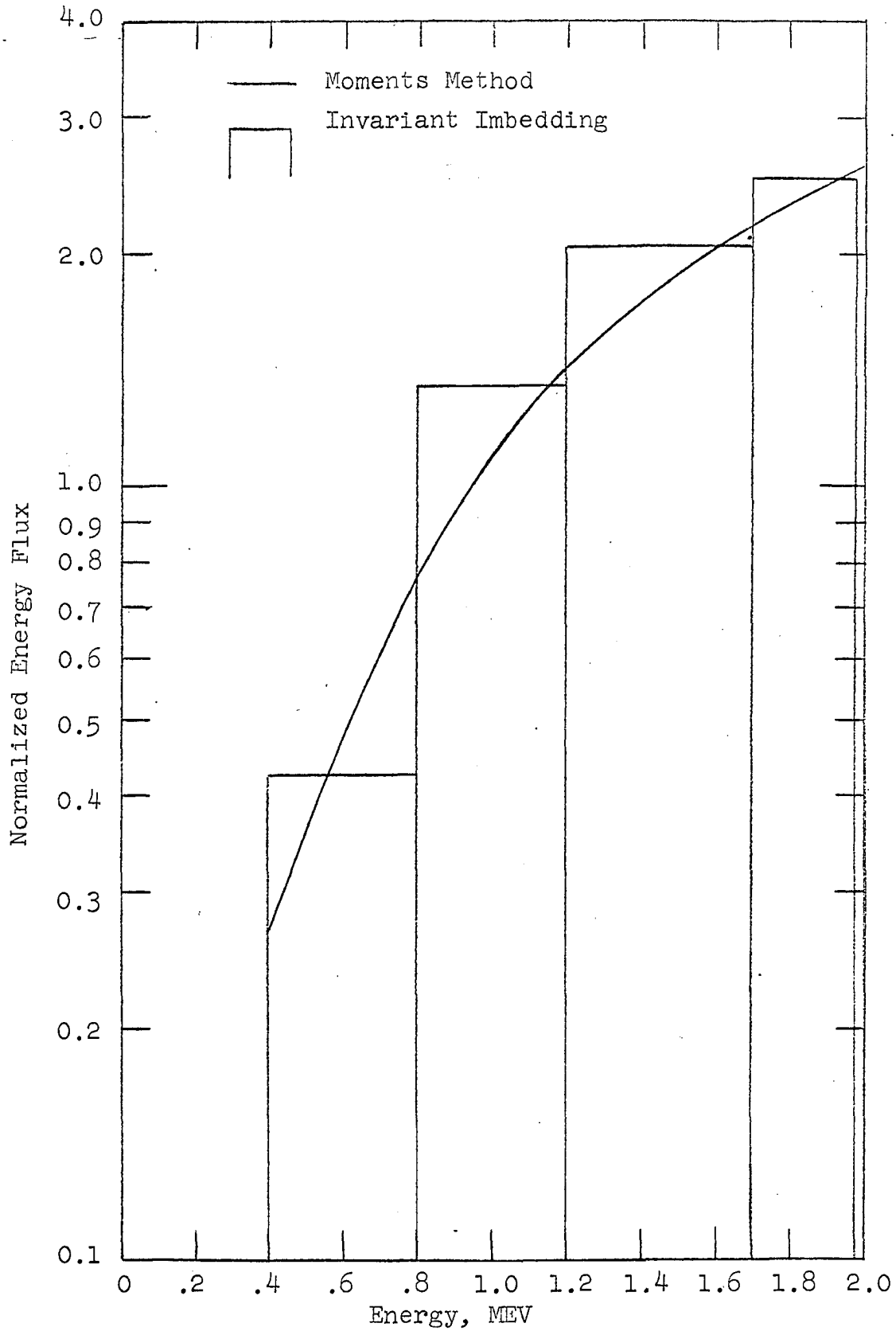
Moments Method
Invariant Imbedding
Normalized Energy Flux
4.0
3.0
2.0
1.0
0.9
0.8
0.7
0.6
0.5
0.4
0.3
0.2
0.1
0
.2
.4
.6
.8
1.0
1.2
1.4
1.6
1.8
2.0
Energy, MEV

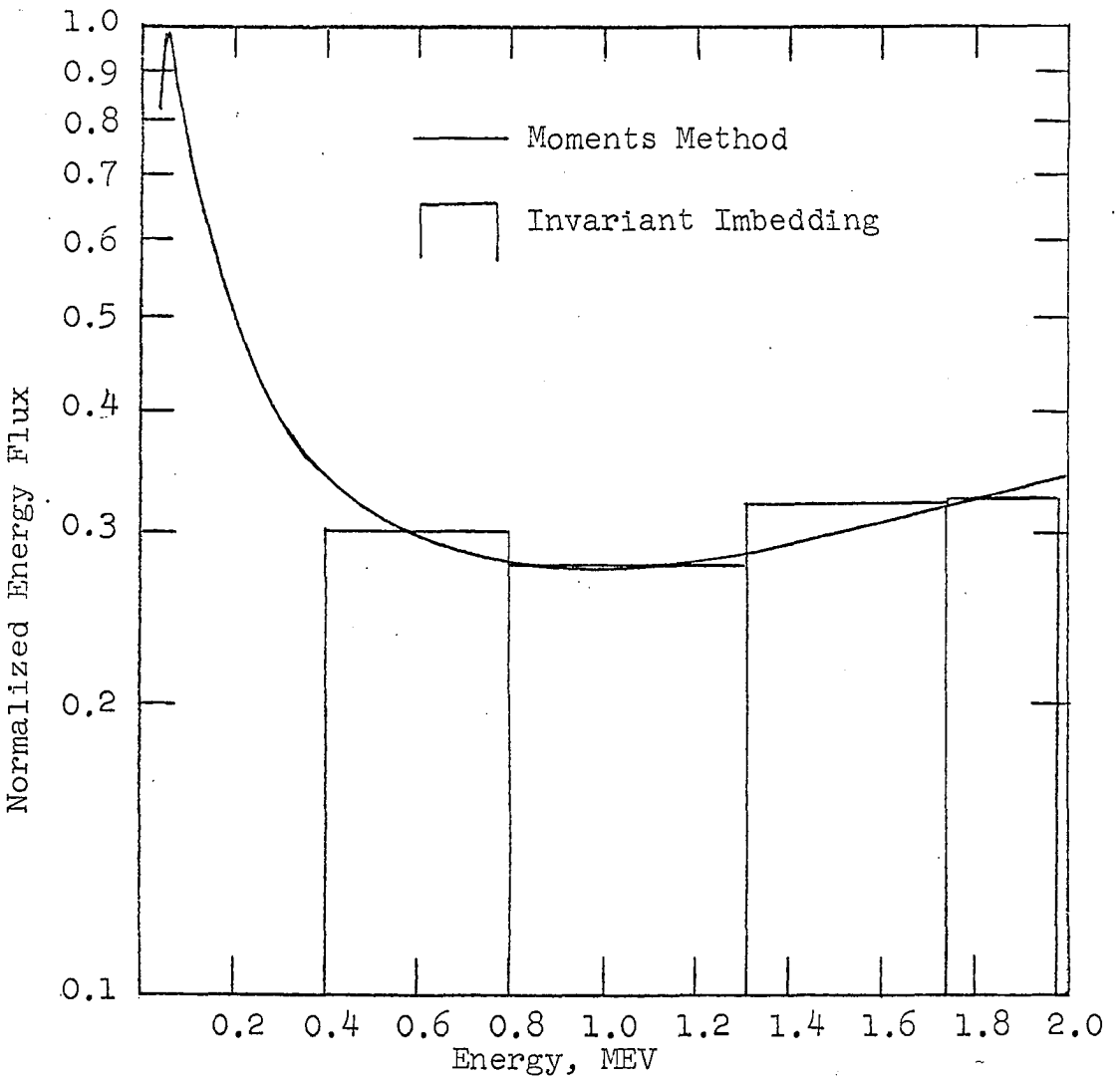

Figure 16. Differential energy spectrum for two MEV gamma rays transmitted through four mean free paths of water

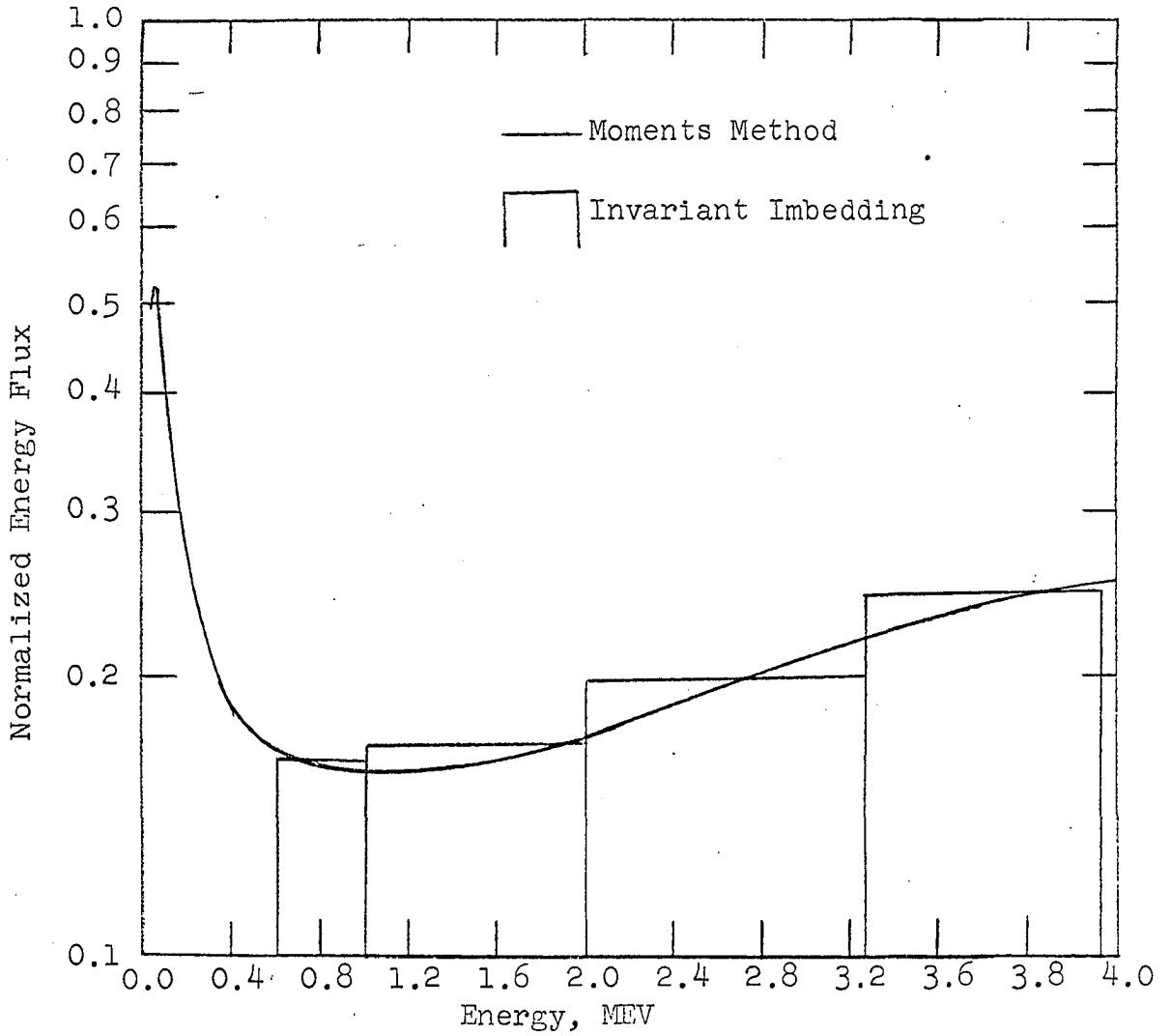

Figure 17. Differential energy spectrum for four MEV gamma rays transmitted through four mean free paths of water

well with those calculated by the moments method. Some difficulty arises in the calculation of the complete spectrum of low molecular weight materials. There is a large pile up of transmitted energy at the low end of the energy spectrum. This is seen if Figures 16 and 17 for the transmissions of two and four MEV photons through water. A large number of energy groups would be needed to adequately approximate this type of differential energy spectrum. This problem does not occur in the higher molecular weight materials. This can be seen in Figures 13 through 15 for the transmission of two and four MEV photons through lead and uranium. In these cases 5 energy groups can adequately describe the energy spectrum of the transmitted flux.

Energy buildup factors

The energy buildup factors for lead, uranium and water are shown in Figures 18 through 23. These calculations were made using Equation 4.44. The transmitted energy flux was calculated using the set of Equations 5.1. A two discrete angle five energy group approximation was used for all the calculations shown in Figures 18 through 22. A comparison between two discrete angle five energy group approximation and a three discrete angle four energy group calculation is shown in Figure 23. In all the figures the present calculations are compared to those made using the moments method.

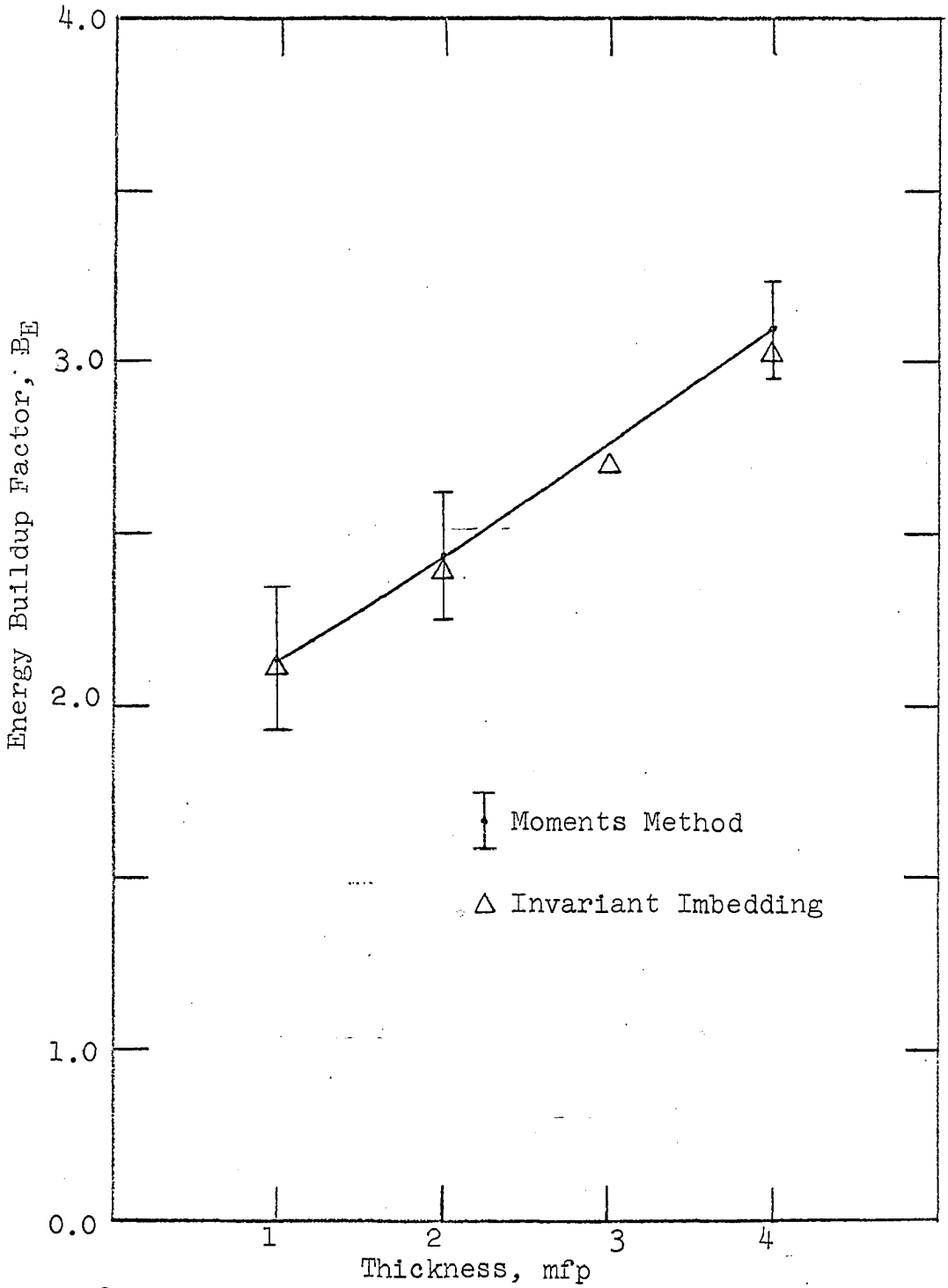

Figure 18. Energy buildup factor for lead due to a two MEV plane isotropic source

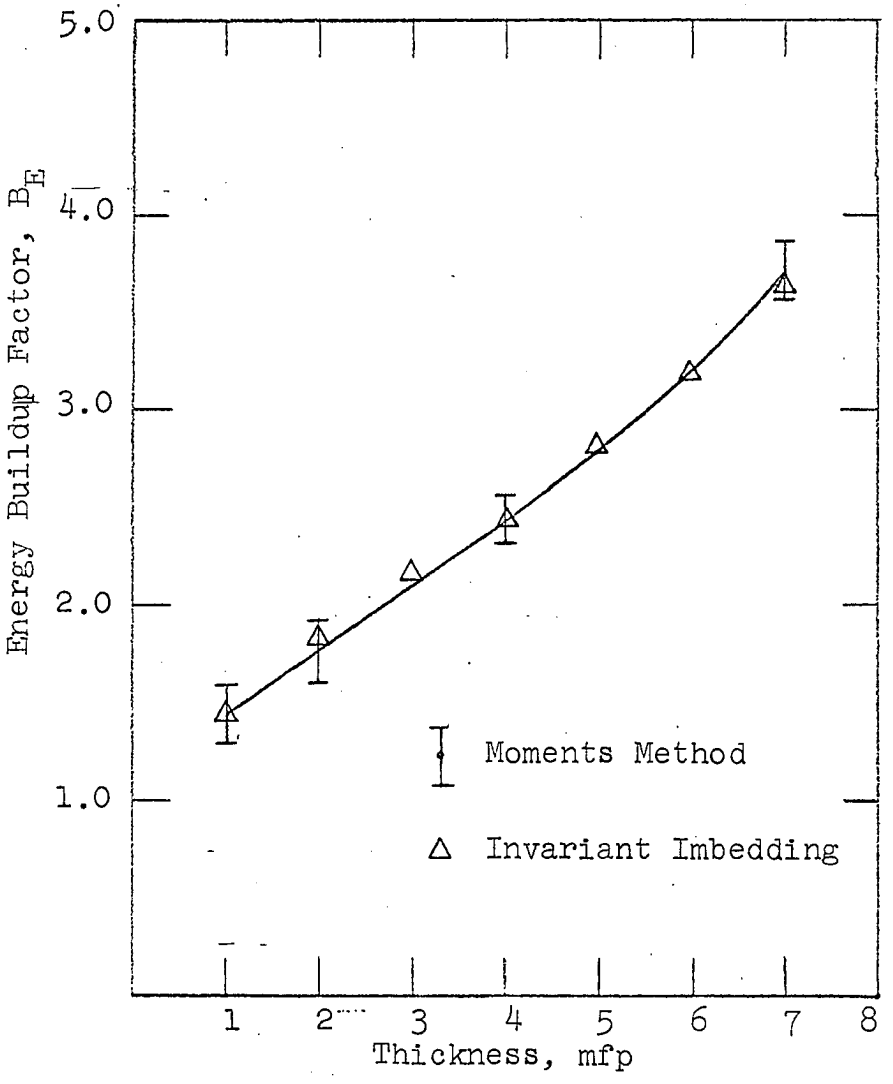

Figure 19. Energy buildup factor for lead due to a four MEV plane isotropic source

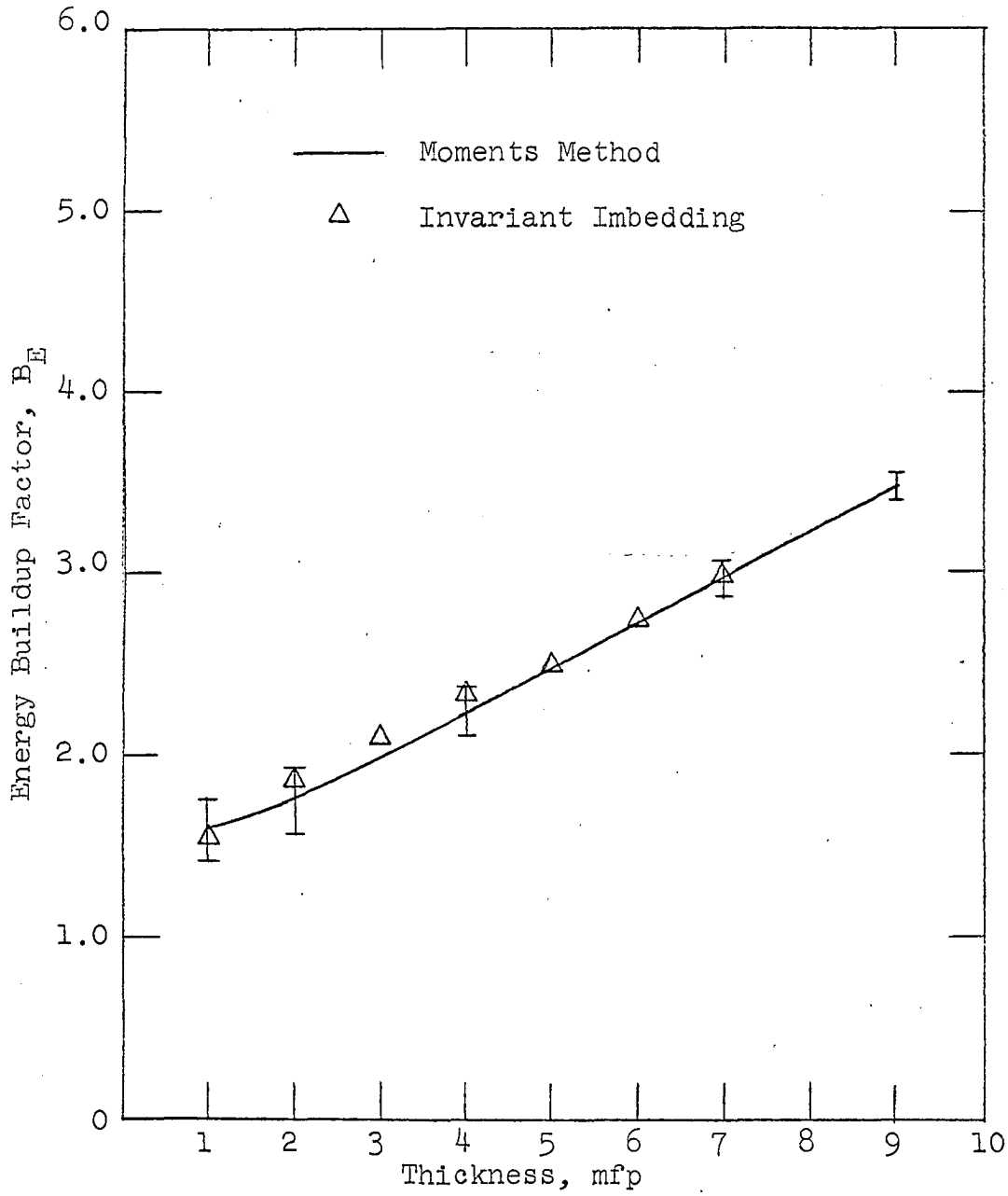

Figure 20. Energy buildup factor for uranium due to a two MEV plane isotropic source

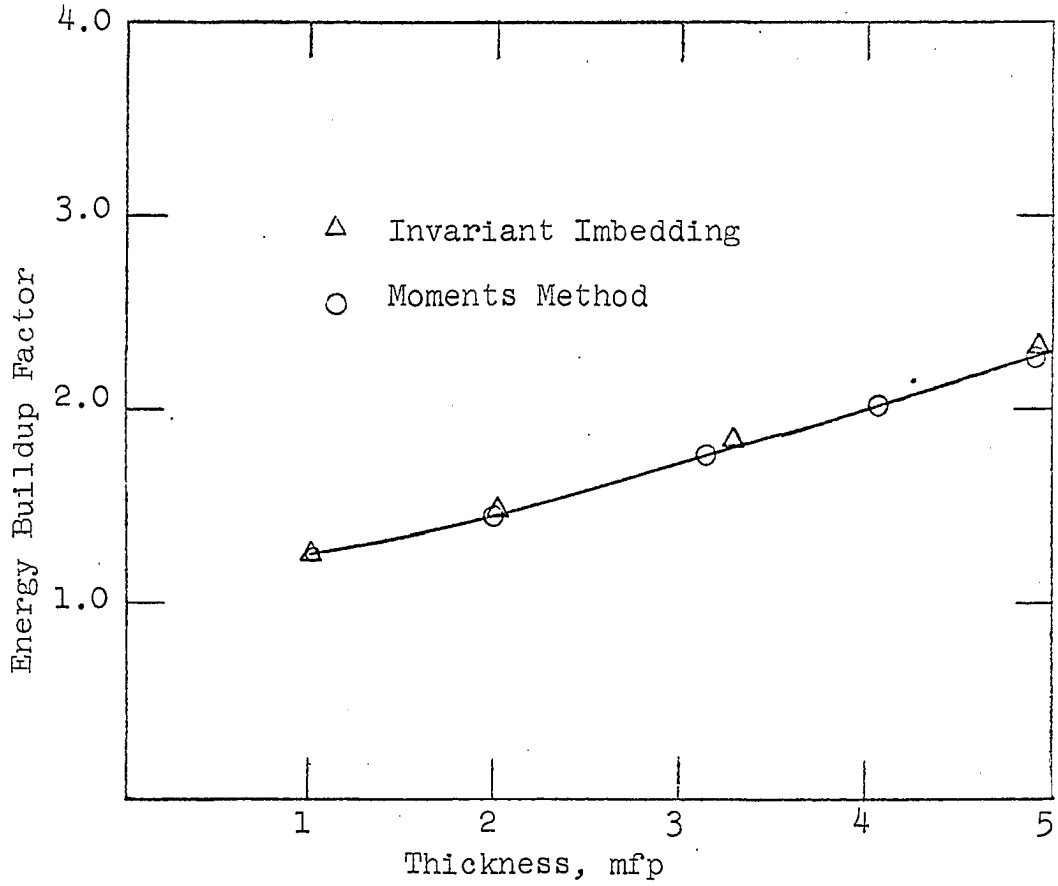

Figure 21. Energy buildup factor for lead due to a four MEV plane monodirectional source

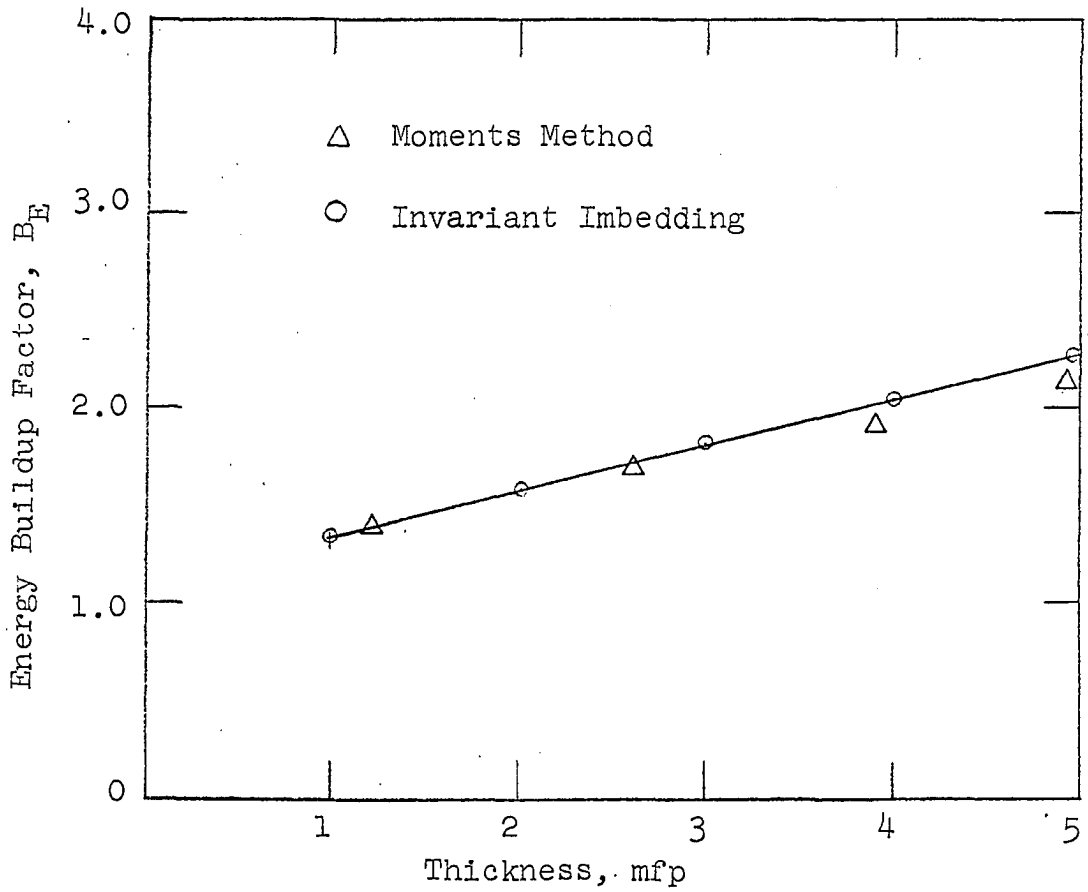

Figure 22. Energy buildup factor for uranium due to a two MEV plane monodirectional source

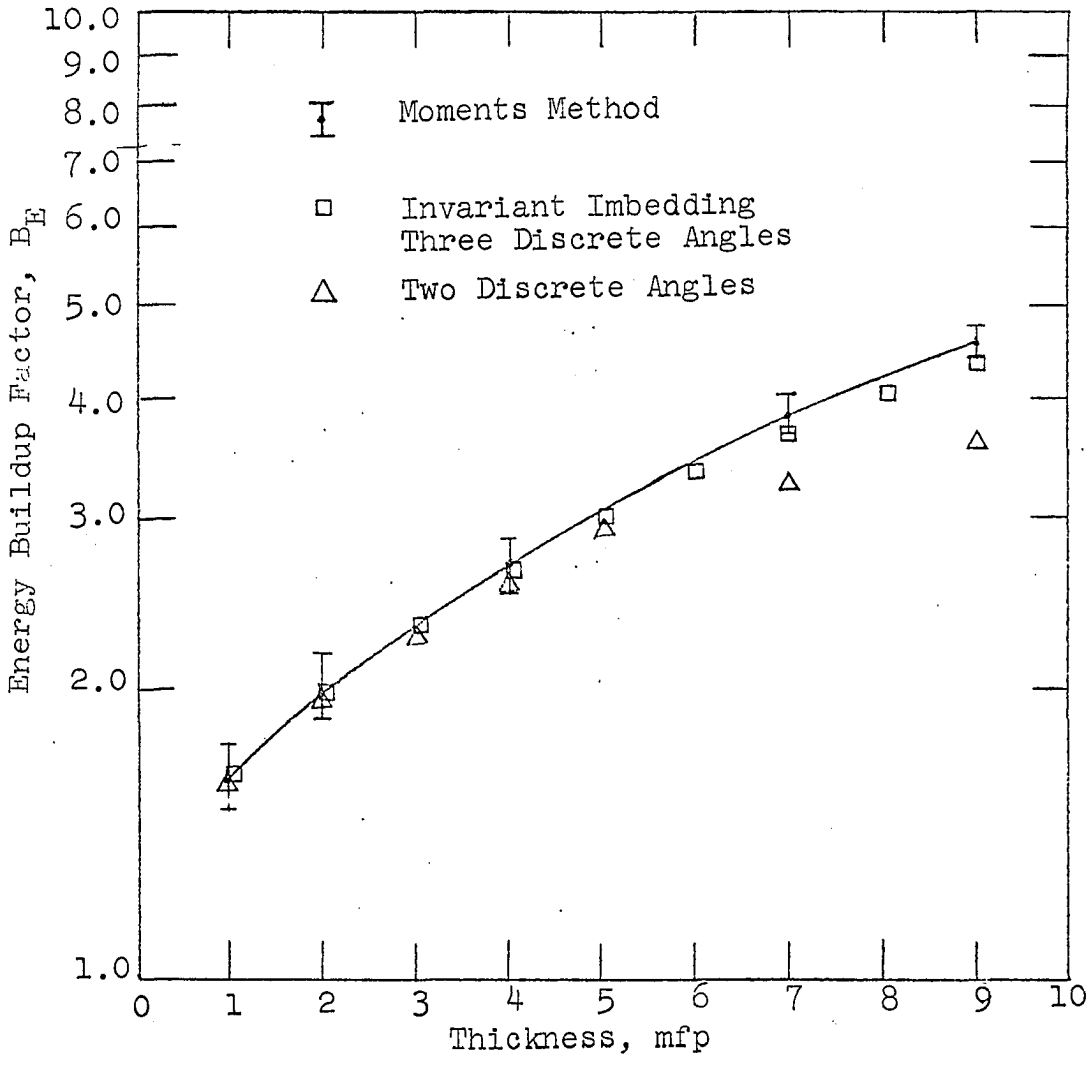

Figure 23. Energy buildup factor for lead due to a two MEV plane isotropic source

In all the calculations where plane isotropic sources were used, the moments method data were obtained by integrating point isotropic source results to obtain plane isotropic source results. This integration introduced some error into the moments method results. The range of accuracy for these results is noted in the figures.

For lead and uranium the energy buildup factors calculated from the energy flux values were found using Equations 5.1. With the two discrete angle, five energy group approximations agree well with the moments method calculations for slab thicknesses to five mean free paths. This applies to calculations using either plane isotropic sources or plane monodirectional sources. The results for plane isotropic sources are shown in Figures 18, 19 and 20 and the results for plane monodirectional sources are shown in Figures 21 and 22. For slabs thicker than five mean free paths the energy buildup factors calculated from the invariant imbedding results are low compared to the moments method results. This is due in part to the low order angular approximations. As the thickness of the slab is increased the angular distributions of the transmitted flux becomes skewed toward the normal. The accuracy of the low order angular approximation becomes worse as the angular distribution becomes more skewed toward the normal. Calculations using two-angle and three-angle approximations are

compared to moments-method calculations for lead slabs in Figure 23. The calculations using the three discrete angle approximations agree with the moments method calculations to nine mean free paths while the calculations using the two discrete angle approximation agree with the moments method calculations to only five mean free paths.

To calculate buildup factors for five slabs greater than nine mean free paths higher order approximations of the angular variations would be necessary. Energy buildup factors for the low molecular weight materials were not calculated because of the large number of energy group needed to approximate the energy spectrum of the transmitted flux.

Evaluation of the numerical method

In all the energy dependent invariant imbedding calculations made for the gamma transport problem, no evidence of numerical instability was found. At no point in the solutions were the values found to be oscillating from step to step. The initial step size used in all the gamma transport calculations was 0.03125. This step size was increased in the asymptotic region to 0.1250 or greater. The execution time for a two discrete angle five energy group calculation to seven mean free paths is less than thirty seconds on the IBM 360/65. A three discrete angle four energy group calculation to ten mean free paths took less than ninety seconds.

CHAPTER SIX. SUMMARY

Numerical and computational techniques were developed to solve the invariant imbedding equations for radiation transport in slab geometry. A computer program was developed using these techniques and calculations were made for the reflection of light in stellar atmospheres, the critical size of a bare multiplying slab and the transport of gamma rays in slab geometry. The values for the reflection of light in stellar atmospheres, calculated using the predictor-corrector method of R. Crane, agreed with values calculated by the Runge-Kutta method to within 0.5%. In all the calculations made using this predictor-corrector method there was no indication of numerical instability. The critical size calculations were compared to calculations made using the S_N method. It was found that the seven discrete angle invariant imbedding calculation agreed with the 16 discrete angle S_N calculation to within 0.1%. The gamma transport calculations were made using invariant imbedding equations that neglect backscattering terms. Energy buildup factors calculates using a two discrete angle five energy group approximation agreed with moments method calculations to within 4% for slab thicknesses to five mean free paths. Agreement to within 4% for thicknesses to nine mean free paths were found using a three discrete angle five energy group approximation.

It is suggested that further applications of the invariant imbedding method to the neutron transport problem and the coupled neutron-gamma problem would yield a significant contribution to shielding theory. The application of invariant imbedding methods to multilayed shields should also be investigated. The predictor corrector method of R. Crane has proven to be well suited for the gamma transport problem and further application of this method to the other suggested shielding problems should be studied.

BIBLIOGRAPHY

1. Ambarzumian, V. A. Theoretical astrophysics, New York, N.Y., Pergamon Press, 1958.

2. Beisner, R. The application of invariant imbedding to shielding problems. U.S. Atmoic Energy Commission Report MR-N-287 (General Dynamics, Fort Worth, Texas). 1962.

3. Bellman, R. and Kalaba, R. Invariant imbedding and radiative transfer in slabs of finite thickness. New York, N.Y. American Elsevier Publishing Company, Inc. 1963.

4. Bellman, R. and Kalaba, R. On the fundamental equations of invariant imbedding. National Academy of Sciences Proceedings 47: 336-338. 1961.

5. Bellman, R. and Kalaba, R. On the principle of invariant imbedding and propagation through inhomogeneous media. National Academy of Sciences Proceedings 42: 629-632. 1956.

6. Bellman, R. and Kalaba, R. Transport theory and invariant imbedding. Proceedings of the Symposia in Applied Mathematics. American Mathematical Society 11: 206-218. 1961.

7. Bellman, R. and Kalaba, R. Invariant imbedding and neutron transport theory. II. Functional equations. Journal of Mathematics and Mechanics 7: 741-756. 1958.

8. Bellman, R. and Kalaba, R. Invariant imbedding and neutron transport theory. III. Neutron neutron collision processes. Journal of Mathematics and Mechanics 8: 249-262. 1959.

9. Bellman, R. and Kalaba, R. Invariant imbedding and neutron transport theory. IV. Generalized transport theory. Journal of Mathematics and Mechanics 8: 575-584. 1959.

10. Bellman, R. and Kalaba, R. Invariant imbedding and neutron transport theory. V. Diffusion as a limiting case. Journal of Mathematics and Mechanics 9: 933-944. 1960.

11. Bellman, R. and Kalaba, R. Invariant imbedding and the reduction of two-point boundary value problems to initial value problems. National Academy of Sciences Proceedings 46: 1646-1649. 1960.

12. Bellman, R. and Kalaba, R. Invariant imbedding, conservation relations and nonlinear equations with two-point boundary values. National Academy of Sciences Proceedings 46: 1258-1260. 1960.

13. Bellman, R. and Kalaba, R. On the principle of invariant imbedding and neutron transport theory. I. One dimensional case. Journal of Mathematics and Mechanics 7: 149-162. 1958.

14. Bellman, R., Kalaba, R. and Wing, G. M. On the principle of invariant imbedding and one-dimensional neutron multiplication. National Academy of Sciences Proceedings 43: 517-520. 1957.

15. Carlson, B. and Bell, G. Solution of the transport equation by the S_N method. International Conference on the Peaceful Uses of Atmoic Energy Proceedings 16: 535-541. 1958.

16. Chandrasekhar, S. Radiative transfer. New York, N.Y., Dover Publications, Inc. 1960.

17. Crane, R. L. Stability and local accuracy of numerical methods for ordinary differential equations. Thesis, Ph.D. Unpublished typewritten manuscript. Ames, Iowa, Department of Mathematics, Iowa State University of Sciences and Technology. 1962.

18. Gill, S. A process for the step-by-step integration of differential equations in an automatic digital computing machine. Cambridge Philosophical Society Proceedings 47: 93-96. 1951.

19. Mathews, D., Hanson, K. and Mason, E. Deep penetration of radiation by the method of invariant imbedding. Nuclear Science and Engineering 27: 263-270. 1967.

20. Mingle, J. Applications of the invariant imbedding method to monoenergetic neutron transport theory in slab geometry. Nuclear Science and Engineering 28: 177-189. 1967.

21. Preisendorfer, R. W. A mathematical foundation for radiative transfer theory. Journal of Rational Mechanics and Analysis 6: 685-730. 1957.

22. Preisendorfer, R. W. Invariant imbedding relation for the principles of invariance. National Academy of Sciences Proceedings 44: 320-323. 1958.

23. Preisendorfer, R. W. Functional relations for the R and T operators on plane-parallel media. National Academy of Sciences Proceedings 44: 323-327. 1958.

24. Ramakrishnan, A. Ambigenous stochastic processes. Journal of Mathematical Analysis and Applications 1: 570-584. 1960.

25. Ramakrishnan, A. Elementary particles and cosmic rays. New York, N.Y., Pergamon Press, 1961.

26. Ramakrishnan, A. and Ranganathan, N. R. Stochastic methods in quantum mechanics. Journal of Mathematical Analysis and Applications 3: 261-294. 1961.

27. Redheffer, F. Remarks on the basis of network theory. Journal of Mathematics and Physics 28: 237-258. 1950.

28. Redheffer, R. Novel uses of functional equations. Journal of Rational Mechanics and Analysis 3: 271-279. 1954.

29. Ueno, S. The probabilistic method for problems of radiative transfer. X. Diffuse reflection and transmission in finite inhomogeneous atmosphere. Astrophysical Journal 132: 729-745. 1960.

30. Ueno, S. The probabilistic method for problems of radiative transfer. XI. On the scattering and transmission functions of S. Chandrasekhar. Annales d' Astrophysique 22: 1-7. 1959.

31. Ueno, S. The probabilistic method for problems of radiative transfer. XIII. Diffusion matrix. Journal of Mathematical Analysis and Applications 4: 21-37. 1962.

32. Ueno, S. On the principle of invariance in a semi-infinite inhomogeneous atmosphere. Progress of Theoretical Physics 24: 734-740. 1960.

33. Wing, G. M. An introduction to transport theory. New York, N.Y., John Wiley and Sons, Inc. 1962.

ACKNOWLEDGEMENT

I wish to thank Dr. A. F. Rohach and Dr. Glenn Murphy for their assistance with the work presented in this thesis. A special thanks goes to my wife, Linda, whose support and encouragement helped make this thesis a reality.